Magma Flow and Interaction with Waste Packages in a Geologic Repository at Yucca Mountain, Nevada

Bruce D. Marsh (bmarsh@jhu.edu)
M.K. Blaustein Department of Earth and Planetary Sciences, Johns Hopkins University, Baltimore, MD, USA

Neil M. Coleman
U.S. Nuclear Regulatory Commission (NRC), Advisory Committee on Reactor Safeguards, Washington, DC, USA

Abstract. The likelihood that a nuclear waste repository at Yucca Mountain could be intersected by igneous activity is very low, but its potential consequences are nevertheless important to performance assessments. An ongoing critical area of concern is the nature and magnitude of the thermal interaction of magma with tunnel walls, high-level nuclear waste packages, and waste forms. Previous assessments consider a variety of dynamic scenarios, but large uncertainties remain in understanding the rheological nature of the magma likely to be involved and its behavior within a repository drift. Here we specifically address the issue of magma rheology during degassing, cooling, and solidification as basaltic magma approaches Earth's surface and enters a drift. Magma containing significant amounts (>~2 wt.%) of dissolved water (Wet Magma), as is anticipated for this region, at or near its liquidus temperature and saturated with water at 200 MPa is at a temperature *near or below the 1-atm solidus temperature*. Isentropic ascent from this near liquidus temperature promotes extensive solidification and/or glassification. Exsolving water with approach to the surface promotes rapid vesiculation leading to fragmentation and tephra production. With continued ascent the still water-saturated magma traverses the solidification phase field and undergoes a combination of rapid crystallization and quenching, becoming a glassy highly viscous (~10^8 Pa s) mass of greatly reduced mobility. This immobility is reflected in the high effective viscosity regulating flows from nearby cinder cones associated with wet basalt. This also matches well with the experimentally determined rheology of dry basalt glass. This rheology greatly restricts the mobility of basalt within repository drifts, amounting to < 10 m per day. Magma in this state quenches rapidly (~10 cm/ min.) on waste packages. Wet basalt is explosive, but relatively immobile as lava. Dry Magma is not explosive, but highly mobile as lava. Previous studies have tended to use an inconsistent set of mixed magma properties involving both extremes. The net effect of our results is that the portion of a repository hypothetically affected by invading magma is likely to be minimal and the number of waste packages affected may be very small. Moreover, the waste packages and/or waste materials affected will most likely be encased in quenched magma.

1. Introduction

Here we examine some consequences of magma entering subsurface drifts containing packages of radioactive waste within a nuclear repository that could be built at Yucca Mountain, Nevada. This is the proposed geologic site for the United States's permanent storage of spent fuel and other high-level radioactive waste (HLW). Of all the many technical factors involved in establishing and sustaining this repository, the potential for future igneous activity to occur, intersect, and compromise the underground facility remains unresolved. This not only involves

estimating the probability of magmatic activity occurring at this location over the next 1million years, but also the complicated issue of the possible damage to waste packages (hereafter WPs) by magma and the transport of waste (i.e., remobilization) to the surface and subsequent dispersal. Nearby volcanism in the form of alkali basalt cinder cones occurring within the past 100,000 yrs is ample evidence that these issues warrant careful consideration.

Analysis of past volcanism (including plausible locations of buried basalts) indicates the probability of a dike intersecting the repository is low at 10^{-8}/yr to 10^{-7}/yr (Geomatrix and TRW, 1996; Connor et al., 2000; Coleman et al., 2004); although some studies from a wider regional perspective place it at least ten times higher (Smith and Keenan, 2005). An update (SNL, 2008) of the 1996 probabilistic volcanic hazard assessment has yielded the following aggregate annual frequencies of repository intersection by any igneous feature: mean = 3.1×10^{-8}; median = 8.7×10^{-9}; and 95th percentile = 1.2×10^{-7}. The probability that a cone-forming vent (i.e., volcanic conduit) could intersect the repository and entrain waste is lower than for a dike because the cross-sectional area for vents is much smaller than for dikes. Nevertheless, despite the overall low annual probability of occurrence, the ensuing implications of magma involvement are being considered in evaluating relative risk to future populations.

1.1. Scenarios for Volcanic Intersection. It is important first to define some possible scenarios for volcanic interaction with the repository. The consequences for future radiological exposures vary significantly among these scenarios (see Figure 3, to be discussed later).

1.) This involves the intersection of the repository drifts by a volcanic dike. As discussed herein, genesis of tephra at the points of intersection and the effects of magma flow and solidification within drifts are important aspects of this event.

2.) Here a conduit-like feeder intersects the drift and connects to a tephra cone-forming volcanic vent on the surface. The transition from flow in dikes to vent flow occurs early in an eruptive sequence, and vents form under various conditions. In low-viscosity basalts, the transition may occur when narrow parts of the dike freeze followed by mechanical and thermal erosion of wider sections as the flow is repartitioned (e.g., Bruce and Huppert, 1990) or alternatively local viscosity variations become amplified by cooling, which concentrates the flow (Wylie et al., 1999). A key difference between a cylindrical volcanic vent and a dike is that the vent cross-section is much smaller (diameter generally <75 m) than for a 1-5 km long dike. Given a field of repository drifts spaced at >50 m, a vent could intersect as a direct hit only one drift along with a relatively small number of waste packages within the cross-section of the vent.

3.) A third scenario for dike-repository interaction involves magma from a dike entering and moving along a drift and enveloping and perhaps damaging a large number of WPs. After filling a drift, it is possible that magma might create enough pressure to generate, at a considerable distance from the intersection point, a secondary dike to the surface (Woods et al., 2002). This so-called "dogleg" scenario, whereby drifts become magmatic conduits, could potentially affect a large number of waste packages, depending on how far the magma travels before final venting. The key factor here is the ability of the magma to fill the drift quickly enough to escape solidification and re-pressurize it to the extent of nucleating a new dike in the drift roof in spite of the initial flow continuing to the surface.

Although our results are applicable to all three of these scenarios, it is most pertinent mainly to the processes of magma flow within drifts and interaction with WPs. We especially focus on the extent of magma penetration into drifts and the potentially critical effects of magma quenching and solidification on WPs and drift walls. The importance of gaining a detailed

understanding of these scenarios, and appreciating the possible mitigating effects of quenching and solidification, can also be appreciated from the point of view of estimating potential radiation doses associated with magmatic activity.

1.2. Current Treatment in Performance Assessments. The largest hypothetical radiation doses arise if extrusive igneous activity occurs during the first 1000 yrs after repository closure (Mohanty et al., 2004, Figs. 3-45 & 3-46). After that time potential doses to future generations diminish significantly because substantial fractions of shorter-lived radionuclides will have decayed. Waste packages should be least degraded during the first 1000 years and therefore most resistant to igneous thermal/physical effects.

Apparently due to the complexity of the processes involved, neither the NRC (Mohanty et al., 2004) nor DOE (2003) trust evaluations of magma-drift-waste package interactions in any detail. They instead assume that a small number of waste containers are completely destroyed upon any contact with magma and the contents carried to the surface via a volcanic conduit (cone-forming vent). The NRC staff currently assumes that such vents will have an average diameter of ~50 m (Mohanty et al., 2004). If the center of a vent coincides with the axis of a drift, then ~5 waste packages are entrained within the cross-section of the conduit and potentially transported to the surface. Nevertheless, it is as yet unclear how or whether the Alloy-22 waste packages or the ceramic or glass waste forms themselves would be reduced to particles of respirable size, as is currently assumed by the DOE and NRC staff.

A detailed, quantitative understanding of the processes involved in magma encountering and interacting with the drifts and WPs is clearly of significant value in overall repository performance assessment, and a great deal of work has been done in this area.

1.3 Intrusive Volcanism and Drift Collapse. The issue of intrusive volcanism is intimately linked to assumptions about the timing and extent of drift collapse. Some investigators have assumed, based perhaps on overly permissive analyses, that thousands of waste packages will be damaged by hypothetical magmatic intrusion of the repository (e.g., Woods et al., 2002; NRC, 2007). However, the presence of backfill in drifts, either intentionally placed or resulting from drift-roof collapse, is beneficial from the standpoint of intrusive volcanism because it blockades the drifts, minimizing the number of waste packages that could be affected. NRC (2007) provides module descriptions and a user guide for NRC's current version of its performance assessment code for Yucca Mountain. In this report and its supporting documentation (NRC, 2007; Ofoegbu et al., 2007; Ibarra et al., 2007), the estimated time for complete (99%) degradation of repository drifts is less than 1500 years. This has major implications for volcanism scenarios because assumptions about igneous intrusion must be consistent with assumptions about drift collapse. Apart from the immediate vicinity of a dike or conduit, drifts would not generally be susceptible to magma influx after they had filled with rubble. Therefore, if it is believed that drifts could fill with rubble in less than 1500 years, then the repository would be susceptible to magmatic intrusion for only a tiny fraction of the repository performance period. This fractional period would be ~1500 yrs / 1 Ma ≈ 0.0015, or 0.15% of the million-year performance period. These insights should be incorporated in performance assessment calculations that relate to the probability of volcanic intersection of a repository and the number of waste packages that could be affected. This makes scenarios involving vast pervasive magmatic flows even less likely, apart from the fact that, as considered

in more detail below, these analyses are commonly based on implausible assumptions about magmatic conditions and properties.

The presence of backfill does not significantly change the volcanism extrusion scenario because these events are likely to entrain only the intersected waste packages and the backfill in the immediate vicinity. The number of waste packages affected this way is small (~5 or less per conduit), based on assumptions about the size distribution for hypothetical intersecting volcanic conduits (e.g., uniform distribution of 5-50 m; NRC, 2007). A substantial fraction of any waste transported to the surface in this scenario may become entombed in lava flows and scoria within a cinder cone, thereby protecting it from erosion for hundreds of thousands of years. Such entombed waste would contribute little to future human dose.

The forthcoming analyses presented below address magma-repository interactions during the first few thousand years after repository closure when waste drifts remain substantially open. This period may well be the time of maximum possible vulnerability of the repository to the effects magmatic invasion.

2. Previous Key Work

As is well known, there has been a huge volume of valuable quantitative work on the problem of magma at Yucca Mountain. Here we only touch on work that is most pertinent to the present study of magma invading a repository drift. The aim is to not only give a background, but to emphasize areas in the past treatment of magma dynamics needing additional work.

Comprehensive reports involving dike-drift interactions have been produced by DOE (e.g., DOE, 2004) and EPRI (e.g., 2004, 2005). These reports consider many aspects of the dynamics of dike propagation, magma flow into drifts, magma-WP interactions, and subsequent WP-aqueous interaction. For magma flow into a drift, DOE uses various coupled models, analytical and numerical, of fluid flow from the dike to the drift. The magma has a viscosity of 10-40 Pa s, and a typical drift of length 150 m is filled in about 15 minutes. Effects of solidification on magma rheology is mentioned, but not explicitly included in flow modeling. This analysis suggests that WPs may be softened, deformed, and corroded by the flowing magma, but not be easily moved, and glassy waste forms are unlikely to be significantly altered by the magma. Yet because of the many uncertain facets of the process encountered in this investigation they conclude that (p. 6-111): “On balance, it would be proper to adopt the conservative position that all waste packages and associated drip shields that come in contact with basalt magma immediately fail.” And in the final application for licensing DOE (2008; p. 2.3.11-10) comes to the conclusion: “Lacking a demonstrated natural or engineered means to limit magma flow from intersected to non-intersected drifts, the intrusion case assumes that, if intersection occurs, all waste packages in all drifts will be contacted by magma and damaged to the extent that they provide no protection for the waste.”

EPRI (2004) analyzed an extrusive release scenario for Yucca Mountain and concluded that the waste package, if intact and still strong, can provide a significant barrier to inhibit the volcanic release of radionuclides. They analyzed several failure mechanisms, including a direct hit on a WP from below, and found reasonable expectation that no waste packages would fail. EPRI (2004) therefore concluded that the expected consequence of an igneous extrusive event would be zero releases of radionuclides to the atmosphere. They did note that waste packages

located directly within a magmatic vent could conceivably contribute radionuclides during the Strombolian stage of an eruption.

Use of more reasonable (to them) assumptions in EPRI's (2005) work lead them to de-emphasize the importance of igneous scenarios in estimating probability-weighted peak doses. They suggest that DOE and NRC may have used so many compounding conservatisms in their evaluations that igneous scenarios have taken on greater apparent risk importance than is justified. They conclude that present DOE and NRC assessments of repository performance are conservative, and reliance on more realistic scenarios and input data would demonstrate an even greater margin of compliance. Based on the results of two summary reports, EPRI (2004; 2005) reached the overall conclusion that there is reasonable expectation that an intrusive or extrusive igneous event at Yucca Mountain will not result in dose levels exceeding the levels anticipated for a base-case scenario with no igneous event, and that no further work need be pursued to address the igneous scenarios.

A key aspect of the EPRI (2005) analysis concerns the realization that magmatic eruptive temperatures are apt to be much lower than they (and DOE) have previously assumed. This stems from experimental phase equilibrium studies on basalt from nearby Crater Flat by Nicholis and Rutherford (2004). This work suggests that, although the magma was at or near its liquidus temperature, because of the magma water content this temperature was much lower than previously assumed (i.e., ~1000°C vs 1150-1200°C). Based on this lower temperature EPRI (2005) used the viscosity-temperature relations of Lore et al. (2000) to estimate a much larger magma viscosity of 10^5 to 10^7 Pa-s. The inherent difficulty with this approach is that the relation shown by Lore et al. (2000) is based on experiments for water-free melts and glasses and cannot be used, as is, through the temperature scale alone for hydrous magmas. Even though the new temperature is much lower, the fact that it is at the liquidus of a water-rich magma, means that the viscosity will be as low (or possibly lower) than that initially assumed by EPRI and DOE. The correlation and regression given by Lore et al. (2000) is, nevertheless, useful as an overall indication of magma rheology from melt to glassy lava, but it does not capture the detailed changes due to crystallinity, water content, bubble content, and bulk composition within the liquidus-solidus range for magma in general. (Magma rheology will be considered again in some detail below.)

As mentioned already, Woods et al. (2002) also analyzed the case in which magma diverts along multiple emplacement drifts and into the main access drift from where it vents to the surface. They conclude that intersected drifts quickly fill with magma, and that a large number of waste packages could be affected. They suggest that prolonged magma flow through the repository, enveloping and bathing the waste packages, over days to months leads to failure of waste packages and provides a mechanism to transport waste to the surface. They did not consider the effects of solidification on rheology or of quenching on WPs. They also suggested the possibility of a shock wave being generated as an ascending dike suddenly breaks into the drift, which then propagates through the drifts. The ideal experimental situation by which to produce a shock wave is to puncture a diaphragm separating a fluid under high pressure from a space at much lower pressure. Disruption of the diaphragm produces a pressure wave with a discontinuity in pressure at its leading edge.

Shock waves have indeed been recorded in volcanic eruptions at well-established central volcanoes associated with island arcs such as at Nguaruhoe in New Zealand (Nairn, 1976) and Mt. St. Helens (Reed, 1980). Shock waves have not been observed during venting of a dike in establishing a fissure-style eruption. The basic structure of island arc stratocone volcanoes,

however, makes them ripe locations for shock wave production. Stratocone volcanoes almost always emit magma from a central summit vent. Korovin volcano on the island of Atka in the Aleutian Islands, for example, has such a cylindrical vent about 300 m wide and 1 km deep that has been observed periodically to be empty and later brimming with magma (Marsh, 1990). Should the summit area become plugged with congealed magma, which is commonplace, rising magma along with the inevitable exsolution of volatiles will overpressure the volcano until it suddenly ruptures. Moreover, many highly explosive island arc volcanoes erupt high crystallinity magma that is near the point of critical crystallinity (~55 vol. %: Marsh, 1981) where the magma becomes a shear resistant dilatant solid, forming an excellent plug at the summit. Merapi volcano in Indonesia is a clear example of this condition (e.g., del Marmol, 1989; Hammer et al., 2000). Thus, large volcanoes repeatedly issuing magma from a central summit vent are, in essence, almost ideal shock wave generators. A dike entering a drift at Yucca Mountain is distinct from this occurrence.

A propagating dike is a magma-filled elastic crack. The leading edge of the dike is literally knife-like and the width of the dike increases slowly away from the tip. Although this is sometimes difficult to calculate in highly fractured country rock with complex elastic properties, examples are available from field occurrences. For example, in the north wall of the east end of Wright Valley in the McMurdo Dry Valleys, Antarctica, the leading edge of the dike associated with the emplacement of the 300 m thick Basement sill is fully exposed (Marsh, 2004; 2007). Over a distance of about 5 km the dike thickness increases progressively from 1 cm at the leading tip to 300 m. A dike intersecting a subsurface cavity or drift will gradually open to its full thickness. Rapid quenching of (most probably) low crystallinity magma along all margins will further impede the rate of opening so that the pressure release will not be catastrophic, as in puncturing a diaphragm, but will ramp-up over a finite time and not allow development of a discontinuity in the pressure field.

The scenario analyzed by Woods et al. (2002) creates a shock wave because of the way the problem and simulation is set up. The imposed initial conditions (both geometric and dynamic) essentially presuppose the solution. But it is the magma physics *before* the assumed initial conditions that actually determines the outcome. The proper portrayal of this part of the problem (e.g., the gradual opening of a leaky fracture into a cavity) precludes formation of a shock wave. DOE (2004) and EPRI (2004) also analyzed the possibility of generation of a shock wave and found magma-drift interactions to be far less severe than those hypothesized by Woods et al. (2002).

The numerical analysis by Dartevelle and Valentine (2005) builds on the Woods et al. (2002) approach but includes full time dependence, 2-D geometry, and a multiphase flow of steam and pyroclastic particles. Although this work has attractive features in time dependence, spatial deposition of particles, and spatial dependence of flow speed and pressure, it also suffers in its fixed (i.e., non-time dependent) 2-D geometry. A shock wave forms at the outset in response to the fixed geometry and the assumed initial conditions of the pressure contrast between the dike flow and the drift.

Detournay et al. (2003) present a comprehensive discussion of igneous consequences at Yucca Mountain, including the potential interactions between a basaltic dike and a repository. In their opinion, the probability that a violent erupting mixture could follow dog-leg conduits is small and more than offset by the degree of conservatism built into the existing estimates. They recommended that a number of new analyses be made, including development of a coupled 3D

model for unsteady dike-drift flow for the scenario of a drift being intersected by a vertical dike and that experimental studies be made on the chemical and mechanical effects of basaltic magma on waste packages in drift and conduit flows.

Overall, we agree that significant conservatisms exist in the DOE and NRC analyses of igneous scenarios. These exist, in a large part, because of major uncertainties in the understanding of the interaction of magma with the repository, and much of this centers on the problem of the thermo-viscous state of magma as it undergoes solidification. For example, Woods et al. (2002) assume that magma moving through a repository drift remains isothermal with "water-like" flow characteristics. This is based on the assumption that magma flow rates will be rapid (10s to 100s m/s; i.e., 20-200 mph) and the thermal inertia of the flow will be large as in flow in a lava tube. But repository drifts are small (~5.5m) with cool walls (100-300°C) and lava quenches and stagnates on all it touches. By not considering realistic scenarios for the thermal interaction of magma with tunnel openings, waste packages, and tunnel walls, there is a real possibility of missing important processes that may not only have implications for understanding other processes (e.g., entrainment and eruption of waste), but also in correctly sensing the overall seriousness of the magma disruption process itself. A prime example in previous work is the serious omission of the exceedingly common phenomenon of magma solidification and quenching. A detailed justification for this opinion is given below after first describing the physical situation.

Figure 1. ----------near here

3. Analysis

3.1 Physical Setup. A depiction of the anticipated form of a typical drift containing waste packages is shown by Figure 1. The drift contains cylindrical waste packages (~1.7 x 5.2 m) resting on cradles and covered from above by drip shields. The design calls for extensive farms of drifts of this nature constructed at a depth of 250-350 m. Each drift is anticipated to be 650-800 m long, separated by about 50 m from neighboring drifts, and interconnected at each end by access drifts, which will be back-filled with crushed stone thereby isolating each drift containing waste packages (Harrington, 2007).

The waste itself is in the form of small cylindrical pellets (~1x2 cm) contained in long slender rods housed in box-like packages and stacked within the canister (Fig.1). The detailed dimensions of the waste packages vary somewhat depending on the exact reactor type in which it was employed.

Temperatures anticipated at the surface of the WPs and within the closed repository (drip shield, drift wall) over 10^5 years, due to the presence of the nuclear waste, are shown by Figure 2. The maximum temperature anticipated is about 180 °C on the waste package, and the drift wall is 10-20 °C cooler.

Figure 2. ----------*near here*

Over the very long (~10^6 yrs) expected lifetime time of the repository, it is possible that the WPs may degrade due to unforeseen factors and the contents, in the form of rods and/or

pellets, may eventually end up as piles of loose material on the floor of the drift. With this in mind, we anticipate four general igneous scenarios involving magma interacting with the WPs at early times when the WPs are fully intact and at late times when the canister housing has disintegrated. These four scenarios are shown schematically by Figure 3. Scenarios Ia and IIa involve an ascending dike or fissure making a direct hit on a WP or pile of waste material. Scenarios Ib and IIb involve magma entering and flowing along the drift, encasing WPs or piles of waste material. Ia has been analyzed in some detail by EPRI (2004, p. 104). Scenario Ib has, in essence, been assumed by the DOE and the NRC under the conservatism of 'taking no credit' for the integrity of the WPs upon interaction with magma. This approach has been resorted to in light of the possible complex and apparent unpredictable response of the waste package to magma interaction. The assumption is that upon interaction with magma "the waste package and associated components would no longer provide protection" (DOE, 2004, section 6.4.8.1). The primary interest of the present work is the latter two scenarios (Ib and IIb), where magma enters the drift and interacts with the WP. We also mention where appropriate certain aspects of the other two scenarios. The so-called 'Dog-Leg Scenario' is also depicted, which is in essence an extension of scenarios Ia and IIb in that the magma travels a significant distance in the drift, ingesting waste, and then venting again to the surface.

It is within this context that we consider the behavior of magma as it enters and flows into the repository drift. Among a host of secondary characteristics, there are two primary aspects of magma that have not been fully explored in the context of magma entering the Yucca Mountain Repository. These are the innate quality of extruding magma to quench on all that it touches and the importance of the near-surface P-T eruptive trajectory on magma rheology. Each of these features involves the fundamental and critical relationship between crystallinity, temperature, volatile content, and rheology, which we now consider.

Figure 3. ----------***near here***

3.2 Magma Crystallinity. The magma-type historically associated with the Yucca Mountain region is alkali basalt. Under surface pressures, it begins to melt at about 1000°C (*solidus* temperature) and with continued melting maintains a rigid structure until the amount of melt exceeds about 50% (vol.) whereupon it becomes a highly viscous, gooey mush of crystals and melt. Continued melting produces a pure, crystal-free, melt at about 1170°C, at the *liquidus* temperature. Conversely, in the cooling sequence once magma exceeds, in the strictest sense, a crystal content of about 50% it is no longer mobile, but becomes rigid immobile rock. At this amount of crystallization (i.e., ~50-55% vol.; the point of *critical crystallinity*) the solids are at close packing and begin to weld to one another forming a rigid network. With approach to this point the viscosity increases almost without limit. In Hawaiian lava lakes, for example, this crystallinity marks the transition from rigid, drillable crust to mushy, sluggish magma (Wright and Okamura, 1977). It also defines the critical concept of magmatic solidification fronts, which exist at the margins of all magmas (e.g., Marsh, 1981; 1996; 2000; 2007). These general characteristics of magma are shown in Figure 4 for a common Hawaiian basaltic magma along with the alkali basalt from Lathrop Wells near Yucca Mountain; this is the same Lathrop Wells composition used in the experimental study by Nicholis and Rutherford (2004). In a more practical sense, with approach to this 50% critical crystallinity barrier the viscosity increases so

strongly that magma becomes immobile at crystallinities nearer 40%. A local loss in temperature of about 100°C along with the attendant crystallization will, thus, for all practical purposes, fully immobilize the magma. If cooling is extremely rapid, as in quenching against cold objects or possibly by rapid de-volatilization, the available melt may become glass, preventing the production of solids, which may curtail the absolute cataclysmic increase in viscosity. Glass formation may, however, depending on the longer term cooling process, be only temporary as crystallization proceeds within the glass itself. Massive glass formation is much less likely in basalts than in more silicic magmas. Possible variations in viscosity for scenarios involving glass formation are also schematically illustrated in Figure 4; more on the rheology of glassy magma will be discussed later in **3.4**.

All magmas erupting on Earth have temperatures below their liquidus and thus always contain some crystals, however few. During the later stages of ascent, prior to imminent eruption, adiabatic expansion promotes cooling, regardless of heat loss to the surroundings, which also promotes crystallization. Moreover, if the magma contains volatiles, like H_2O and CO_2, which are common constituents of alkali basalts, the dramatic loss of these volatiles with approach to the surface (i.e., drop in pressure) progressively shifts the governing phase diagram to higher temperatures (see below). This promotes massive crystallization and quenching, which most often takes the

Figure 4. ----------***near here***

form of swarms of needle-like crystals of feldspar (plagioclase) in glass. Because magma near and on Earth's surface is always undergoing crystallization, magma quenches against virtually anything it touches. Foreign fragments of rock (xenoliths) entrained in magma commonly show quenched magma around the margins, even those from as deep as the mantle. In Hawaii, for example, magma quenches against and around trees (Figure 5), and on cars and trucks. Heated sap bursts the trees and the trees often catch fire, burning away to leave a hollow vertical pillar in the lava.

Figure 5. ----------***near here***

All magmas moving as dikes through fissures near Earth's surface show strongly quenched edges in all contacts with the host rock. These ubiquitous features are called 'chilled margins.' The basic physics of this process is straightforward. In attempting to heat the material with which it is in contact, the magma loses a critical amount of heat that brings it to a solid or glassy state. The overall process is very much akin to the behavior of molten paraffin, which at its liquidus when spilled quenches against all that it touches, even cooler blocks of paraffin. The perception that magma will continue to 'run' past and continually bathe a waste package in a well-mixed bath of magma is a critical oversimplification. Only, possibly, if a waste package were dropped into a vertical column of low crystallinity (i.e., near liquidus) magma and allowed to settle hundreds of meters would such a situation be roughly approximated, and even then quenched

margins would form on the package. It is important to realize that magma in the near surface is continually cooling. There are no normal means by which magma can acquire heat, it is chilled and cooled by everything it touches, including the atmosphere. The heat produced by crystallization (i.e., latent heat) occurs in response to cooling, slowing, but not normally reversing, the cooling process; limited heating during volatile-loss induced crystallization is possible (see below).

3.3 Quenching of Magma on Waste Packages. The melting point of Alloy 22, from which the waste package casing is manufactured, is in the range of 1350-1380 °C. The container itself, although significantly above the temperature of the ambient drift wall rock due its radioactive contents, will be much cooler (<~200°C) than any invading magma. Quenching will be especially effective against the waste packages because of the large thermal conductivity of metal (see Table 1 and Appendix I), which greatly facilitates heat transfer and causes the principal thermal resistance to reside in the magma. Quenching forms a glassy rind of a thickness that can be calculated from knowledge of the waste package (hereafter WP) thermal inertia or enthalpy and its size.

Using conservation of energy, we equate the sum of the thermal energy of the system before and after quenching. The goal of this analysis is to estimate the thickness of the quenched rind that forms on the WP, and this will be followed by an estimate of the time taken to form a quench rind of this thickness. The total thermal energy before (LHS below) and after quenching (RHS below) is the sum of the enthalpy of the WP and the associated quenched rind (hereafter QR). That is,

$$(\rho Cp\, V\, T_o)_{WP} + (\rho Cp\, A\, d\, T_m)_{QR} = (\rho Cp\, V\, T_C)_{WP} + (\rho Cp\, A\, d\, T_q)_{QR} \qquad (1)$$

where V is WP volume, A is WP surface area, d is the QR thickness, ρ is density, Cp is specific heat, and T is temperature with subscripts: T_o for initial WP temperature, T_m initial magma temperature, T_C contact or interface temperature between WP and magma, and T_q average temperature in the QR. Because the magma will quench to mainly glass the role of latent heat has been ignored unless otherwise noted; the effect of latent heat on the contact temperature will be treated below. And since we expect the QR to be relatively thin the approximation V = Ad has been assumed above for the QR volume. It should also be clear that we assume, as a maximum effect, that the full volume of the cooler WP is the heat sink that cools, in effect, a concomitant volume of magma. In essence, the WP is treated as a large xenolith encapsulated by lava. The physical properties and the initial WP and magma temperatures are known, the thickness (d) and the average temperature (T_q) of the QR are unknown.

The thickness (d) of the quenched rind can be found from (1)

$$d = \left[\frac{(\rho Cp)_{WP}}{(\rho Cp)_m}\right]\left(\frac{V}{A}\right)\left|\frac{(T_C - T_o)}{(T_m - T_q}\right| \qquad (2)$$

The initial temperatures of the WP and magma relative to the temperature necessary to quench the magma are clearly important. If, as an unrealistic extreme example, the magma temperature must be reduced to the initial WP temperature, which must then also be the temperature at the WP-magma contact, then $T_q = T_o = T_C$, and d=0. There is no quench rind. On the other hand, if

quenching occurs after only a very small temperature drop, then $T_m \sim T_q$ and d becomes very large. It is clearly important to consider possible estimates of T_q and T_C relative to T_o and T_m.

T_q can be estimated from knowledge of the contact temperature (T_C) on the surface of the WP. The contact temperature T_C can be found through an energy balance similar to (1) above performed over an arbitrarily thin region at the contact

$$T_C = \frac{T_o(\rho Cp)_{WP} + T_m(\rho Cp)_m}{(\rho Cp)_{WP} + (\rho Cp)_m} \tag{3}$$

For common properties (Table 1) this reduces to

$$T_C = 0.45T_o + 0.55T_m \tag{4}$$

which very nearly reduces to the well known result from many general studies of magma cooling (e.g., Jaeger, 1968; Marsh, 1989). That is,

$$T_C \approx \frac{T_o + T_m}{2} \tag{5}$$

which will be used henceforth.

To be more explicit, using an exact solution to the heat conduction equation, the contact temperature (T_C) at one side of a sheet embedded in an infinite wall rock medium is given by $(T_C\text{-}T_w)/(T_o\text{-}T_w) = (1/2)[\mathrm{erf}(2L/(4\kappa t)^{1/2})]$ (*Carslaw and Jaeger*, 1959), where T_o and T_w are, respectively, the initial sheet and wall rock temperatures, erf is Gauss's Error Function, t is time, and κ is thermal diffusivity. For small times, the erf argument becomes large and $\mathrm{erf}(2L/(4Kt)^{1/2}) \sim 1$, and the maximum contact temperature is $T_C = (T_o + T_w)/2$, which is (5) above. The result is exactly the same for any hot sheet buried within a cooler medium or even a hot sheet on Earth's surface (e.g., see Fig. 4 of Carslaw and Jaeger, 1959). If the effect of latent heat is also included within the hot sheet, the exact solution for the contact temperature is $(T_C\text{-}T_w)/(T_o\text{-}T_w) = (1/[1+\mathrm{erf}(b)])$ (e.g., Marsh, 1989, eqs (38) and (45)), where $b = (C_p(T_o\text{-}T_w)/5H(\pi)^{1/2})^{2/5}$ and C_p is specific heat and H is latent heat. For typical basalts, b~0.6 and $T_C = 0.62\ (T_o + T_w)$, but this assumes complete crystallization and for partial crystallization, as is closer to the present consideration, the result (5) above is sufficient; also note that in the limit of large b, which would hold for small H, this also reduces to (5). If the effect of curvature of the cylinder is included the factor becomes less than 1/2 (*Carslaw and Jaeger*, 1959). This result also holds if the magma is flowing past the WP. That is, for a fully-developed flow the fluid streamlines for this highly viscous magma will locally be approximately parallel to the contact and normal to the direction of heat flow, the advective term in the full heat equation will be identically zero (i.e., $V \bullet \nabla T = 0$).

Overall, (5) is a fairly robust result and the contact temperature is thus approximately the average of the initial WP temperature and the magma temperature. For a WP at 100°C, for example, and magma at 1100°C, the contact temperature is 600°C. Moreover, this is the maximum temperature attained, and this temperature is sustained at this value until cooling reaches the center of the hot body whereupon the contact temperature recedes slowly with time as long as heat is also eventually lost from the WP to the floor rock of the drift (e.g., Jaeger, 1968; Marsh, 1989).

Table1. Physical Properties of Basaltic Magma (rock) and Waste Package Material.
(See Appendix I for more specific values at specific temperatures and for references.)

Parameter	Value
Drift diameter	5.5 m
Drift length	650-800 m
WP diameter	1.6-1.7 m
WP density	4067-3602 kg/m^3
WP thermal conductivity	16.4-19.5 W/m-°C @500 °C
WP specific heat	485 J/kg-°C @500 °C
WP thermal diffusivity	4.5-4.67 x$10^{-6}$$m^2$/s @~500 °C
Magma density	2500 kg/m^3
Magma thermal conductivity	1.818 W/m-°C
Magma specific heat	900 J/kg-°C
Magma thermal diffusivity	0.8x$10^{-6}$$m^2$/s

If the entire QR must be reduced to the contact temperature (T_C) for quenching, substitution of (5) into the last group of (2) gives

$$d = \left[\frac{(\rho Cp)_{WP}}{(\rho Cp)_m}\right]\left(\frac{V}{A}\right) \qquad (6)$$

It may be somewhat surprising that this result does not explicitly involve the relative initial temperatures of the magma and the WP, but these effects are embedded in the results above for T_C and T_q. The QR thickness depends mainly on the ratio of WP volume to surface area (V/A), which for a cylindrical WP of radius R, reduces (6) to

$$d \approx 0.41\,R \qquad (7)$$

where the areas of the WP ends have been ignored.

There are also other, less severe, approximations for the temperature (T_q) of the QR. If a linear increase in temperature is assumed across the QR from T_C at the contact to T_m at the outer margin, then

$$T_q = \frac{T_C + T_m}{2} \qquad (8)$$

And using (5) and (8) in the last term in brackets in (2) again gives,

$$d = 2\left[\frac{(\rho Cp)_{WP}}{(\rho Cp)_m}\right]\left(\frac{V}{A}\right) \qquad (9)$$

which is twice the thickness for the case when $T_q = T_C$.

Judging from these reasonable extremes for estimates of T_q, the possible thickness of the quenched rind on the WP will be on the order of the radius of the WP itself. That is, the rind will potentially be in the range of about 0.5 to 1 meter. Since the package is not a solid mass of metal, some allowance has been made in this estimate for the effective mass of the waste package, for the rate of internal heat transfer, and the possibility of a higher heat capacity due to the presence of a silicate glass in the waste pellets. Nevertheless, since the internal packing assembly holding the waste pellets forms a 3-D grid or conductive circuitry, internal heat transfer may be relatively rapid. The above estimates are for the final, long-term cooling effect of the WP in forming a quenched rind. We next consider the time taken for this quenched rind to develop and then turn to ways in which it might be resorbed**.**

The time (t_q) to grow this quenched rind will not be instantaneous and will be given approximately by

$$t_q = (C\sqrt{\kappa})^{-2}\, d^2 \qquad (10)$$

where d is the thickness of quenched rind (cm), κ is the thermal diffusivity of the magma (~10^{-2} cm^2/sec), and C is a constant. This equation can be found by scaling the diffusion equation of heat conduction or also by solving the classic Stefan problem for solidification (Carslaw and Jaeger, 1959; e.g., p.285, eq.(12)) And this specific result is well calibrated from measurements of the solidification rates of Hawaiian lava lakes and lava (Wright and Okamura, 1977; Mangan and Marsh, 1992; Hon et al., 1994). The time of quenching is shown by Figure 6 as calculated from (10) where the group of constants is given by,

$$C\sqrt{\kappa} = 1.87 \times 10^{-4}\, T - 6.58 \times 10^{-2} \qquad (11)$$

where T is any particular isotherm in °C and the units are cm-$s^{0.5}$ or for units of m-$hr^{0.5}$,

$$C\sqrt{\kappa} = 1.12 \times 10^{-4}\, T - 3.94 \times 10^{-2} \qquad (12)$$

The time to grow a 3 cm thick quenched rind is ~10 sec, while an 8 cm thickness of rind will grow in ~1 min. A 0.5 m thickness of rind, which might be expected from the purely thermal balance results above would grow in ~1 day, which is consistent with the rates of solidification of Hawaiian lava flows. There are many examples of this quenching process.

Figure 6. ----------*near here*

A relevant example of this process of quenching is well demonstrated in a series of massive experiments conducted by Sandia Laboratories in the late 1970's in an attempt to understand the extraction of thermal energy from molten magma using an inserted heat exchanger (e.g., Hardee, 1975; Fewell et al., 1975; Hardee and Fewell, 1975). The basic setup was a barrel-like cylindrical vat holding 0.2 m^3 of Hawaiian basalt maintained by induction heating in a superheated state of 1450 to 1650 °C. (This is 250 to 450 °C *above* the basalt liquidus, and much hotter than any lava flow.) A heat exchanger (cylindrical finger or probe ~15 cm diameter made of Type 310 stainless steel) was inserted into the vat of magma and the efficiency of heat transfer to steam within the probe was monitored. Even though the basalt was maintained at an extreme temperature through constant heating, which forced the melt to vigorously convect, a quenched

rind of glass always formed on the probe. Because of the extreme and unrealistic continuous external heating, it is not possible to compare the rind thickness (~2 cm) to that predicted above, which is for a melt than can only cool. It does suffice to show, however, that quenching will clearly occur even under the most extreme conditions.

Perhaps a more pertinent example is MacCulloch's Tree in Ardmeanach of the western Mull magmatic complex of Scotland (Emeleus and Bell, 2005). Here a large (~2 x 15 m) upright Eocene (~55 Ma) conifer (*Taxodioxylon*) has been encased in a columnar basalt lava flow. The clearly defined quenched margins are of a thickness approximately that of the radius of the tree (see Figure 7). In addition to the distinct quenched margins, also clear in this example is notable horizontal columnar jointing or fracturing due to contraction upon cooling. Columnar jointing is an indicator of the direction of cooling, with the trend of the columns being in the direction of the local strongest influence on cooling. This pattern of jointing shows the major effect of this tree in quenching massive flowing basalt.

Figure 7. ----------*near here*

Figure 8. ----------*near here*

Even at high temperatures when xenolithic (i.e., foreign) wall rock is caught up in ascending basalt the effect of quenching can also be significant. Shown by Figure 8 is an ultramafic nodule caught up in alkali basalt from the San Bernadino volcanic field in SE Arizona. This basalt is similar to that erupted from the Crater Flats volcanic field just to the west of Yucca Mountain. A clear quench rind is present on much of the nodule; some of the adjoining vesiculated basalt may also be due to quenching. What makes this of special interest is that the nodule is spinel peridotite, which characterizes the upper mantle just below the continental crust. This suggests that this small xenolith was only slightly cooler than the host basalt and was transported a significant vertical distance of perhaps 20 km without losing the quench rind due to prolonged heating in a large bath of magma. Nevertheless, that the quenched rind is thin or missing over part of the nodule may indicate the direction of relative settling of the nodule in the less dense basalt during ascension. Yet it is also possible that the shroud of vesiculated material attached to the nodule may also be due to quenching. And, we hasten to point out, that should a xenolith be incorporated into magma undergoing massive quenching, as during H_2O-depressurization (see below), there will be no obvious quench rinds as the entire assemblage on a much larger scale, perhaps many meters, would be the effective quench rind.

A final example is the common practice of geologists at the Hawaiian Volcano Observatory to get samples of flowing lava by tossing a steel hammer on the end of a long wire into the flow and immediately pulling it back out with a large clump of lava quenched on the hammer.

Taken altogether these examples, in effect, substantiate the above estimates for the magnitude of the effect of quenching of magma and lava on cool objects. It is important to appreciate that all terrestrial lavas are erupted at temperatures *below* their liquidi and any local cooling whatsoever will cause crystallization and/or glass formation (see below).

3.4 Magma Rheology. As mentioned already, the question of the number of WP involved in an eruptive event centers, in part, on the length of drift exposed to magma. If the eruptive material is pyroclastic debris, a local small subsurface cinder cone will, in effect, form and quickly plug the drift through avalanching and welding. On the other hand, if the eruptive is low viscosity (e.g.~10^2 Pa s) lava, a significant distance of drift may become involved. The flow of lava through a drift can be estimated by assuming flow through a pipe whose radius shrinks in time due to magma solidification around the margins of the drift. To be clear, this is only an approximation, albeit a reasonable one, as the true flow is a flow entering an empty pipe where the avalanching front (i.e., in the fashion of a tractor tread) is an important feature at the earliest times (also see later). A prime difficulty in performing such calculations is in the proper choice of the viscosity and, more specially, the general rheological state of the magma as **it** approaches Earth's surface as magma and then as lava. We first consider the lava viscosity and, then, using this insight, broaden the analysis to the possible rheological state of the magma itself as it approaches the repository level.

Given the magma composition, temperature, volatile content, and crystallinity, the estimation of viscosity is straightforward using standard methods (e.g., Marsh, 1981; Spera, 2000). Each of these characteristics can be estimated for magma similar to alkali basalt erupted nearby at Lathrop Wells, but there is a major problem in using this approach because the volatile content of the expected basalt changes rapidly with approach to the surface. That is, as will be explained in more detail in the subsequent section, because of the suspected high volatile content, this magma will undergo volatile saturation at depth (~5 km) long before it reaches the surface and will begin devolatilizing and unavoidably solidifying rapidly in approaching the surface. When the degassed magma reaches the surface it will already be near its 1-atm *solidus* temperature (i.e., final crystallization temperature) and will have become, in essence, a glassy paste-like material of enormous viscosity. If the magma were to rise slowly under complete chemical equilibrium as governed by its thermal state, upon reaching the surface the magma would be ~100 vol.% crystals, and its effective viscosity would be beyond about 10^{15} Pa s. That this does not happen, and that the magma becomes a high temperature mixture of tiny crystals and glass, reflects the inability of the kinetics of crystallization to keep pace with depressurization (e.g., Marsh, 1998). This is strongly reflected in the extent of the lava flows at Lathrop Wells.

The radial extent of the flow fields at Lathrop Wells (and similarly at nearby Crater Flats) are about 1 km; the volume of the lava field at Lathrop Wells is about 0.03 km^3 (e.g., Heizler et al., 1999; Valentine et al., 2006; 2007). Although the duration of the flow is not known with any certainty, because of the nature of the flow (see below) the magnitude of the viscosity controlling the flow can be estimated. The flow can be approximated as a gravity current of viscous fluid spreading on a nearly flat surface (e.g., Huppert, 1982). This method has also been used to examine lava dome and lava growth associated with the 1979 eruptive event on Soufriere on St. Vincent (Huppert et al., 1982).

Approximating the radial spreading of lava as an isothermal viscous gravity flow is but one of several mechanisms suggested to control lava spreading and lava dome growth (e.g., Fink and Griffiths, 1998; Griffiths, 2000; Lescinsky and Merle, 2005). The strength of the enveloping crust, the internal yield stress, and the role of damming at the toe of the flow may each also dominate the flow at certain stages of growth or stages of cooling. Although the rates of radial growth predicted by the various models are similar, lava dome height over time tends to favor growth controlled by the yield strength of the surficial crust. In terms of revealing an effective

viscosity of the lava itself, however, the various models are mutually exclusive. That is, each model yields a set of physical properties not found in the other models, and additional, more detailed, physical features added to a model often yield a better fit to observation. The viscous model, for example, can be made to fit better if the effect of damming at the toe is larger or if the lava viscosity is significantly larger than that independently estimated from lava composition and temperature. In the latter respect, we show below that, due to the sudden loss of volatiles with approach to the surface, the Lathrop Wells alkali basalt underwent rapid pressure quenching and may well have attained a viscosity much larger than otherwise expected. Moreover, this viscosity is remarkably consistent with that found from modeling the Lathrop Wells lava as a gravity flow. On these grounds and the fact that only through this model can an estimate of viscosity be found, we prefer to model the spread of lava here as a viscous gravity flow.

The radial extent of the viscous flow of a fixed volume of magma released on a flat surface is given by (Huppert et al., 1982)

$$R = 0.894\left[\frac{gV^3}{3\nu}\right]^{1/8} t^{1/8} \qquad (13)$$

where g is gravity, V is volume, ν is kinematic viscosity (= μ/ρ, where μ is shear viscosity and ρ is density), and t is time. Results from the use of this equation are shown by Figure 9

Figure 9. ----------***near here***

for a variety of viscosities and total lava volume as a function of the duration of the event. For an alternative model of lava issued at a given flux, also due to Huppert et al. (1982), the corresponding results are given by Figure 10.

An additional simple alternative model is for lava of a given thickness and viscosity flowing down an inclined plane as along a gully or other accommodating terrain (Figure 11). Actual lava flow thicknesses at Lathrop Wells may be as much as 15 m, which for an extent of 0.5 km and a duration of several months indicates a viscosity of larger than 10^9 p. It should also be noted that for a much smaller viscosity of, say, 10^2 p, as might be expected for hot, dry and voluminous lavas of, for example, the Columbia River Basalts, the flow by these same calculations would be expected to go great distances, tens of km should the volume be sufficient.

From these collective results and with a maximum flow extent of ~1 km, the apparent effective kinematic viscosity of the lava is in the vicinity of about 10^9 to 10^{10} cm^2/s. The exact duration of this ~80,000 year old flow is not known, but flow events of this nature generally last about a month to a year. The *aa* character itself of these flows suggests a mass flux of about $3x10^4$ kg/s (Wood, 1980), which when used in concert with the observed volume suggests a duration of about 30 days. Alternatively, if the full volume of Lathrop Wells (~0.03 km^3) is assumed to have been erupted over a period of time from between a year and a month, then, the volumetric flux is from about 1-10 m^3s^{-1}. This is a typical flux observed for scoria cones of this general type.

Figure 10. ----------***near here***

A significantly larger viscosity ($2x10^{12}$ poise) was similarly deduced by Huppert et al. (1979)

for Soufriere, which, apparently not believing the result, they ascribed to the influence of a high viscosity skin or quench rind enclosing the lava. Although this skin effect may be important, the fact that the Soufriere lava contains almost 50% (vol.) crystals could also be a major factor in greatly increasing the viscosity (Marsh, 1981), making the originally derived result possibly realistic. Using an approach based on the Jefferys equation, which also describes flow down an inclined surface, Manley (1992) found similar results for the viscosity of blocky basaltic andesite and andesite flows. He noted that these viscosities are some 1.8 to 3.6 orders of magnitude above that predicted for the lava itself based simply on chemical composition and temperature.

There is also direct evidence in the lavas from Lathrop Wells of the petrologic conditions favoring such large estimated values of effective viscosity. This evidence is in the form of the modal concentration of crystals, mainly plagioclase, and glass in the lavas and in the spatial variations in these quantities with distance outward from the central vent. In a suite of samples collected by us radially along the flow, the crystallinity and coarseness of the crystals increase with distance from about 40 vol.% crystals at the vent to about 70 vol.% at the flow terminus (see photomicrographs in Hinze et al, 2008b; p. 124, Fig. 52); some of this could be due to cooling after emplacement. The presence of glass decreases in abundance with distance from the vent and increased cooling and in concert to the increase in crystallinity. Since viscosity becomes effectively infinite when crystallinity exceeds about 55-60 vol.%, the lava fragments into large blocks and may move more as a debris flow than as a viscous fluid; the viscosity of melt squeezing out between the blocks will not be an accurate indicator of the rheology governing the overall flow itself. This fragmentation increases the volume of the lava and when this occurs in a confined space, as in the subsurface or a repository drift, the lava dilates upon shear to plug the vent, stifling further flow. Dilatantcy of this nature is a common property of all granular material (e.g., Marsh, 1981; Marsh, 2007).

Figure 11. ----------***near here***

In all of this modeling, the key feature is the movement of a certain volume of lava over a certain distance in a specific time. At Lathrop Wells, although the initial crystallinity was not large, there is evidence in the blocky fragmentation, steep flow fronts, rafted well-formed vent blocks supported by the flow, and the degassing sequence of the ascending magma (see below) and extrusion of lava that the viscosity was large. This may well reflect the transformation of a preponderance of glass in the final, near surface magma to a large increasing population of plagioclase microlites. The overall impression gained from these considerations suggests that the viscosity governing the flow of this magma and lava is large ($>\sim 10^8$ c.g.s.). This critical condition may be an intimate reflection of the rapid quenching to glass of water-rich basaltic magma as it ascends and rapidly depressurizes, which process is now considered.

3.5 Magma Solidification During Final Ascent. During ascent, magma free of dissolved water (i.e., Dry Magma) cools and solidifies only by adiabatic (isentropic) expansion and conductive heat losses to the wall rock (Fig. 12). The slope of the liquidus of Dry Magma relative to the adiabatic cooling gradient, which is ~0.5 °C/km, shows that any crystals initially present in the magma will begin to melt. That is, without conductive losses during ascent, solidification stalls and is reversed, crystals are melted, and as soon as the magma temperature exceeds the liquidus and becomes superheated vigorous thermal convection will ensue (e.g., Marsh, 1989; Hort et al., 1999; Zieg and Marsh, 2005). Thermal convection rapidly reduces the temperature to the

liquidus where, with the loss of superheat, convection ceases and conductive losses may further drop the temperature and promote crystallization (Winslow and Marsh, 2007).

Figure 12. ----------***near here***

The exact temperature history will clearly depend on the specific dynamics of the ascent history (i.e., V(t)). The inevitable result is that the eruption temperature of a dry magma will, in general, be near the liquidus, which is commonly observed for Hawaiian magmas and deduced through geothermometry for ocean ridge magmas (Marsh 2007). That is, all terrestrial magmas erupt at or below liquidus temperatures; superheated eruptions have never been observed.

For magma containing significant amounts (>~2 wt.%) of dissolved water (Wet Magma), the geometry of the associated phase diagram for the same basalt is much different (Fig. 12). Magma near its liquidus temperature and saturated with water at 200 MPa may be at a temperature *near or below the 1-atm solidus temperature*. Isentropic (adiabatic) ascent from a near liquidus temperature here also causes cooling, which will promote solidification (Harris, 1977; Saghagian and Proussevitch, 1996; Papale, 1997: Mastin and Ghiorso, 2001), but there is a much stronger effect. Because the solubility of water in magma is essentially zero at surface pressures (1 bar), ascending Wet Magma will undergo strong exsolution of water with approach to the surface (the magma essentially gets the bends). Exsolving water promotes rapid vesiculation eventually leading, at vesicle fractions above 70-80 vol.%, to fragmentation of the magma itself (e.g., Navon and Lyakhovsky, 1998). With continued ascent the magma, still saturated with water, traverses the phase field and undergoes a combination of rapid crystallization and quenching to glass. If not for fragmentation and tephra production, whereupon the magma now becomes essentially a continuous gas phase laden with particles of quenched glassy magma, the magma would become a glassy highly viscous mass of greatly reduced mobility (more below). Although Wet Magma clearly can be much more explosive than Dry Magma, once stripped of excess bubbles the still water-saturated magma with continued ascent will become highly viscous.

It is important to note that exsolution of water, in and of itself, will not warm the magma. The viscous dissipation of energy due to the intense shearing of the melt upon vesiculation and fragmentation will warm the magma, but this is bounded by the loss of available potential energy attending ascent. This possible warming is more than offset by the cooling of expansion of the exsolved gas (Mastin and Ghiorso, 2001). Local viscous heating due to shear is clearly possible (e.g., Shaw, 1969; Spohn, 1980), especially in a fragmenting and expanding flow (Mastin, 2005), but in the massive, non-fragmenting regime this effect will be self-regulating, due mainly to continuity effects, and unlikely to be important (Marsh, 1984).

The pre-eruptive water content of typical Lathrop Wells basalt has been inferred by Nicholis and Rutherford (2004) by matching the observed phase assemblage of the lava to that found experimentally under varying water contents in the melt. Nicholis and Rutherford (2004) conclude that the magma was at or near water saturation at a pressure of about 200 MPa (2 kb = ~5.5 km depth), which is also shown on Figure 12. The phase diagrams for the same Lathrop Wells melt composition are shown by Figure 13; the Dry Magma phase equilibria was calculated using the well-known MELTS numerical code (Ghiorso and Sack, 1995), and the Wet phase diagram is from Nicholis and Rutherford (2004) (with additional information also from MELTS) as are the indicated pre-eruptive conditions. A likely eruption path is also indicated. The slight heating indicated with approach to the surface is due to the possible effect of latent heat associated with partial (~25%) crystallization induced by depressurization. The actual ascent P-T

path is uncertain unless the physical means of ascent is known, but bounds can be placed on the path, which is next considered.

If the magma ascends abruptly, undergoing massive vesiculation, expansion, and fragmentation, without allowing the melt to undergo any further crystallization, the melt will cool by about 75°C, which is shown by Figure 14 (Mastin and Ghiorso, 2001). The fragments of magma will quench to a glass containing only the crystals initially present before eruption.

Figure 13. ----------*near here*

Next consider the magma residing immediately below the fragmentation interface. Here the magma is at a degree of vesiculation less than that necessary for fragmentation, but still dominated volumetrically (i.e., 50-70%) by expanding bubbles. Although melt will be carried upward (and perhaps also laterally if the wall rock is sufficiently permeable) by this expanding mass, unquenched melt can also drain from this matrix of bubbles. Further below, at higher pressures and still lower degrees of vesiculation, melt is the dominant phase and individual bubbles can rise and join the overlying medium. The net result of melt draining from the bubble matrix and bubbles 'draining' upward from the melt matrix is a region of devolatilized melt. This melt will still be at vapor saturation and will still adhere to the Wet Magma phase diagram of Figure 13. But if in this process of dramatic volatile loss attending eruption the ambient pressure becomes significantly less than the original hydrostatic pressure, which is likely, as the eruption wanes and the ambient or near ambient pressure regime is reestablished, the residual melt will be left somewhat undersaturated in water. The prevailing phase equilibria will now dramatically shift to something intermediate between the two systems of phase equilibria shown by Figure 13. The net effect is that the melt will undergo spontaneous quenching *in situ* with perhaps some crystallization of a pervasive groundmass assemblage of tiny crystals. This process may oscillate back and forth until a steady state is established by forming a mass of degassed quenched magma moving sluggishly to the eruptive vent. Upon arrival at the surface this magma is essentially a high temperature glass whose temperature has been increased somewhat from latent heat of crystallization. The approximate ascent trajectory is indicated by Figure 13a.

Figure 14 ----------*near here*

A clear example of this process and this style of heating due to crystallization attending depressurization has been recorded by the Mount St. Helens eruptives (Blundy et al, 2006). Glassy fluid inclusions in plagioclase record the P-T-crystallinity ascent trajectory, indicating an ascent path for this dacite magma similar to that already discussed for basalt. The overall phase relations and the determined ascent path are shown by Figure 13b. The dry phase relations have been calculated using MELTS (Ghiorso and Sack, 1995) and the water-rich phase relations are from Rutherford et al. (1985). The beginning ascent point is at a depth of about 6 km where the magma temperature is about 860 (+/-20) °C and the crystallinity is about 30 (+/- 5) vol.%. This temperature is *below* the corresponding dry solidus both at this depth and at 1- atm on the surface, which is at about 880 °C, and the dry, 1-atm liquidus is at about 1185 °C. Upon ascent the magma increases in crystallinity by about 25 vol.%, going from initially 30% to a final crystallinity of about 55%. The heating (ΔT) resulting from this increase of 25% crystallinity

($\Delta\phi$) can be calculated from the effective latent (H~60 cal/gm) and the specific heat (Cp ~ 0.25 cal/gm-°C). That is, $\Delta T = H\ \Delta\phi/Cp = 60$ °C, which is the amount of heating observed.

It is also interesting to note that the final crystallinity is ~55%, which is the critical crystallinity at maximum packing and rheological lockup. Corresponding to these severe rheological conditions, these glassy magmas erupted to form domes of highly limited areal extents. Also noted on Figure 13b are the equilibrium crystallinities in the 1-atm, dry system, which for commensurate crystallinities are at much higher temperatures, indicating the mechanically induced disequilibrium nature of the crystallization attending ascent and extrusion of this magma. It is also emphasized that although this is a dacite magma and not an alkali basalt, the governing process is similar and basalt is expected to behave similarly.

The rheology of an extruding basaltic mass will thus be governed by a glassy microcrystalline medium. The rheological properties of magmatic compositions in the glass state have been examined experimentally by Webb and Dingwell (1990). The viscosities of a spectrum of compositions from rhyolite to nephelenite as a function of strain rate are shown by Figure 15. Although as fully molten magmas at the same temperature the viscosities of these compositions are markedly different, contrasting by about 10^5 p between rhyolite and basalt, as glasses the viscosities of this wide range of compositions are remarkably similar at a value of about 10^{13} p. The temperature of measurement of the basalt glass is 716°C. At a higher temperature of about 900 °C, which would be closer to the eruptive temperature of the Lathrop Wells lava, the viscosity of glassy basalt would decrease to about 10^9- 10^{10} p (i.e., calculated using typical glass activation energies in this work). This value is similar to that estimated earlier by approximating the flow of lava as a viscous mass spreading under the action of gravity. The typical strain rate expected for the Lathrop Wells flows is indicated by the stippled region on the figure, which is less than about $3x10^{-5}$ s^{-1}. This estimate comes from assuming a flow velocity of 1 km for a month (i.e., V~$4x10^{-4}$ m/s) and a vent diameter of 10 m. At this and smaller rates of strain, viscosity is independent of the rate of strain and the viscosity is thus Newtonian. At larger rates of strain the effective viscosity decreases with the rate of strain and the rheology becomes significantly non-Newtonian as a shear-thinning material or thixotropic or even psuedoplastic material (Webb and Dingwell, 1990).

Figure 15. ----------*near here*

With this understanding of the rheology of silicate glasses in mind, it is also notable that a major dissatisfaction in modeling lava and lava dome growth as simply a spreading viscous flow has been that the apparent governing viscosities obtained are much larger than that estimated on purely petrologic grounds. That is, if the viscosity of the Lathrop Wells alkali basalt is estimated at any temperature where it is dry and molten and the crystallinity is relatively low (i.e., <~25 vol.%), the viscosity will be only about 10^2-10^3 p. But if it is a high temperature glass, with or without a similar amount of crystals, its viscosity will be closer to 10^9 p (10^8 Pa s). This dramatic contrast in viscosity may account for the apparent mismatch between modeling results and assumed petrologic conditions defining the state of the extruding magma. Moreover, the brittleness and low tensile strength of subsolidus basalt (see below) make it a poor material to act as a confining layer or elastic membrane to regulate dome and lava growth. This same material, however, being strong in compression, may function well to, in effect, dam and impede the advance of already otherwise sluggish flows. These two factors, unusually high viscosity and

impeded flow fronts, may be critical factors in matching the distance-time and height-time observations that have otherwise found viscous flows wanting (e.g., Griffiths, 2000).

These same factors, in addition to others, may be critical in controlling the flow of magma into the repository drifts.

3.6 Penetration of Magma into Drifts: As discussed already (see Fig. 1), the drifts containing the WPs are circular and the flow of magma along them can be well approximated by flow into an initially empty pipe, albeit with obstructions. Neglecting for the moment the empty pipe effect (i.e., the magma is actually entering an open pipe), the influence of WPs and of possible deposits of scoriaceous debris, there are three primary factors controlling the penetration distance of magma into the repository drifts: Drift radius; Magma viscosity; and Driving pressure gradient. These are summarized in the following generalized equation for the flux (Q) of fluid of viscosity μ moving along a circular pipe of radius a(t) under a pressure gradient of $\Delta P/L(t)$ (e.g., Batchelor, 1967).

$$Q(t) \sim \left[\frac{\Delta P}{L(t)}\right]\left[\frac{a(t)^4}{\mu}\right] \qquad (15)$$

Because of cooling, quenching, and solidification of the magma, the effective radius of the drift decreases with time. Strictly speaking, this also reflects changes in the viscosity field, which will vary radially and downstream in the flow as a function of temperature and crystallinity. This overall effect can be separated into two parts: an outer region of unusually high viscosity, which is locked against flow due to cooling and quenching, and an inner or core region where the viscosity is approximately constant at the initial value. This method of separating the viscosity field into inner and outer regimes to understand the dynamics is well-established (e.g., Morris, 1982).

The overall process is in the nature of the well-known thermal entry effect whereby a hot fluid enters a cool pipe (e.g., Marsh, 1978; Bejan, 1984; Delaney and Pollard, 1982). In entry processes, both the thermal and velocity profiles develop downstream from the entry point. Propagating inward from the walls, each profile develops by diffusion, one by thermal diffusion and the other by momentum diffusion. The time (t) to develop a steady state profile is given approximately by $t \sim a^2/D$, where D is the appropriate diffusivity (κ or ν, as above).

For values of the effective kinematic viscosity of $\sim 10^3$ (c.g.s) or greater, the velocity profile in a drift of 5.5 m diameter will become fully developed in less than about one minute. In light of the expected magnitude of the viscosity discussed earlier, the velocity profile can be assumed to be always fully developed. Although far from the leading edge of the flow the velocity profile may approximate a typical parabolic flow field, near the leading edge the flow moves into the empty drift more like a tractor tread. The front over-steepens and magma avalanches ahead onto the WPs and drift floor. Because of its importance in understanding the behavior of fluids injected into molds, broadly similar problems of this basic nature have been well studied experimentally and analytically (e.g., Frigaard and Crawshaw, 1999; Kolli et al., 2002; Manas-Zloczower et al., 1987; Behrens et al., 1987). If not for the highly probable glassy and fractured state of the entering lava, the fluid just behind the flow front could re-circulate upwards and form a moving eddy at the base of the front. (Possibly picking up debris from the drift floor.) But here the flow front is expected to be more like that of the lavas on the surface, namely, steep and blocky, and shortly (i.e., within several drift diameters) behind the front the flow will

approximate a parabolic flow. Radiative cooling of the flow front will further enhance this process.

The thermal entry effect lasts much longer. For $\kappa \sim 10^{-2}$ (c.g.s.), it takes about four months for the thermal fronts to become fully developed. This thermal effect progresses as treated earlier for quenching (equations (11) and (12)) and is reflected by the changing drift radius a(t).

As is common in many magmatic flows, the pressure gradient ($\Delta P/L$) driving the flow along the drift is the most uncertain parameter in eq. (11); it cannot simply be set or chosen but is, in essence, self-regulated by the flow itself. There are three approaches to estimating this parameter: 1.) If the flow moves as lava on an inclined plane or as a flow on a flat surface that spreads by inclination of the upper surface, the driving pressure gradient is given by $\Delta\rho\ g \sin(\theta)$, where $\Delta\rho$ is density contrast, g is gravity and θ is the dip of either the drift floor or the upper surface of the flow. 2.) If the flow is, in essence, 'pulled' along by the steep avalanching front or the outward slope of the flow surface in general, there is a pressure gradient given by $\Delta\rho\ g\ h/L(t)$, where h is the drift height and L(t) is the distance of the front from the entry point. This is, in essence, a variation on the sloping surface of 1). And last, 3.), perhaps the most extreme approximation is the pressure gradient due to a standing hydrostatic column of magma stretching from the drift to the surface (~300 m), whence $\Delta P/L \sim \Delta\rho\ g\ Z/L(t)$, where Z is the depth of the drift and all else is as before. In this case, for a homogeneous, low viscosity magma the pressure (ΔP) at the base of the column would be ~7.35 MPa (i.e., ~73.5 bars).

The best constraint on these choices is to estimate the effective pressure gradient that operated to erupt the lavas associated with a cinder cone like nearby Lathrop Wells. This can be done by rearranging (15) and finding $\Delta P/L$ as a function of eruptive flux (1-10 m^3/sec), vent size (radius), and magma viscosity. For flow through a pipe-like feeder (15) becomes,

$$\frac{\Delta P}{L} = \frac{8\,\mu\,Q}{\pi\,a^4} \qquad (16)$$

It is clear here that for a given flux, the pressure gradient is directly proportional to magma viscosity and inversely proportional to the vent radius (to the fourth power). That is, the lower the viscosity of the magma the smaller $\Delta P/L$ needs to be to deliver the requisite flux to the surface. Results for $\Delta P/L$ calculated from this equation along with similar estimates from the three models discussed above are shown by Figure 16.

Figure 16. ----------***near here***

The diagonal field of lines marked 'Lava Flux' contains the pressure gradients necessary for fluxes of 1-10 m^3/sec, as estimated earlier for Lathrop Wells, and for vent radii of 5 to 20 m all as a function of magma viscosity. The horizontal lines are the pressure gradients associated with the three models introduced above and are marked 'standing column' for that of a column of magma reaching from the drift to the surface, 'flow front' for the flow pulled ahead by the avalanching flow into an empty pipe, and 'lava flow' for the flow down an inclined slope (upper or lower surface).

The area of overlap between the two methods of estimation is for viscosities of about 10^8 to 10^{10} (c.g.s.), and for a vent size of about 10 m, the pressure gradient given by the 'lava flow'

model and the 'avalanching front' model may agree best unless the effective viscosity is nearer 10^{10} whence the 'standing column' pressure distributed over 100 m of drift length may be better. It is also important to emphasize that for lower viscosities (<~10^8), the requisite pressure gradients indicated by the Lathrop Wells fluxes are much lower than would be predicted by any reasonable standing column of magma. This most likely indicates that a standing column of magma in near hydrostatic equilibrium is an unrealistic model. In this regard, it is also useful to point out that once a vent to the surface is established above the drift, the walls may be permanently deformed and act more like an open, rubble-filled mine shaft or volcanic crater than an elastic medium (more below). Magma rising to the level of the repository drift may thus flow into the drift more like the 'lava flow' or 'avalanching front' models. These two models have a common physical basis when the flow is driven by the slope of the upper surface, which will slope away from the entry point. In this regard, we begin by calculating the flux of magma into a drift where the flow is driven by a slightly sloping upper or lower surface.

The flux of fluid Q along the drift is, following (15), given by

$$Q(a,\mu,t) = \left[\frac{\pi \Delta\rho g \sin(\theta)\,(a - d(t))^4}{8\mu} \right] \qquad (17)$$

where, as above, $\Delta\rho$ is density contrast, g is gravity, a is drift radius, μ is viscosity, d(t) is the inward growth of the quench rind as above, and the upper flow surface or drift floor is assumed to slope away at a slight angle (~5°). This slope is underestimated for an upper lava surface as it enters an empty drift and overestimated for the floor as the intended design places the drift at near-horizontal (~0.3°).

The length of drift filled by lava as a function of time is found by integrating (17) over time for the total volume as a function of time and dividing by the volume of drift per unit distance. This gives,

$$Q_T(a,\mu,t) = \left[\frac{\pi \Delta\rho g \sin(\theta)\, a^6}{120\mu\, f^2} \right] \left[(1 - C(a,f)t^{1/2})^5 (5(1 - C(a,f)t^{1/2}) - 6) + 1 \right] \qquad (18)$$

where C(a,f) = f/a and f is the factor $C\kappa^{0.5}$ in equation (11) above. Results calculated from this equation are shown by Figure 17 as a function of lava viscosity, drift diameter, and duration of flow.

Figure 17. ----------***near here***

For the viscosities governing the Lathrop Wells lava field (~10^9 c.g.s.) and for effective drift diameters of 3-4 m, where allowance has been made for the presence of WPs partially obstructing the drift, lava penetration over a ten-hour period will be on the order of a meter. For an effective viscosity of 10^7, over a ten-hour period the flow will penetrate about 3.5 m for an effective 3 m drift diameter.

Although perhaps less realistic, for purposes of comparison the penetration distance when the pressure gradient is from the standing column of magma extending from the repository to the surface is given by Fig. 18. Strictly speaking, the full problem should be solved where the pressure gradient decreases in concert with the depth of penetration over the time of the flow into the drift, which is analytically tractable. But to emphasize the strong effect of this pressure gradient, the driving pressure has been taken as a constant for each flow situation, but the characteristic distance over which the pressure acts has been varied in the example calculations (see Fig. 18).

Figure 18. ----------***near here***

The strong effect of the pressure gradient is clear in these results. As L, the drift distance over which the differential pressure acts, decreases and the pressure gradient thus increases, penetration distance for any viscosity increases strongly. For a magma viscosity of 10^8 Pa s and L = 100, the penetration distance is about 35 m. If L is increased to 1000 m, as judging from Fig. 15 may be reasonable, penetration decreases to less than 5 m, and if L further increases to about 3000 m, as for a lava flow, the penetration distance is only a few meters or less. If viscosity is decreased to 10^7 Pa s and L = 500, the magma penetrates about 70 m into the drift. In the actual process the driving pressure will decrease in response to the evolution of the flow.

Others have also noted the difficulty in estimating this governing pressure gradient. Detournay et al., (2003) discuss this is some detail and mention the possibility that, because of the porous and permeable nature of the wall rock, the leading edge of the ascending magma-filled dike (after the dike has been established) may be at or near atmospheric pressure at the level of the drift. This would make the dynamics of inflow more akin to a lava flow. They go on to estimate this driving pressure by relating it to the head of magma above the drift that results from the interaction of the ongoing dike flow and magma loss into a series of drifts.

The best estimate of the drift penetration distance comes from a careful and full consideration of a specific eruption scenario and not simply from an isolated calculation detailing a specific physical part of the entire process. For example, any eruption is most likely to commence as a gas-rich tephra and agglutinate-laden Strombolian phase. This will deposit, and possibly plug as discussed already, a great deal of material in the drift at the intersection with the dike. As this Strombolian phase wanes and dense magma approaches the surface and reaches the level of the repository, the magma may well lack sufficient driving pressure to reach the surface all at once (as observed at Paricutin), and it may flow into the repository drift as a lava flow. The overlying dike to the surface will be filled with porous tephra and agglutinate, the dike walls would suffer permanent (i.e., unrecoverable) deformation, as mentioned above, and the overpressure may approach atmospheric pressure at the repository depth of 300 m. That is, the overlying dike may be structurally more like an open mineshaft than a fluid-filled column under hydrostatic pressure. The presence of pre-existing deposits of tephra will greatly subdue the effective pressure gradient driving the magma laterally and will also act as a granular plug to stifle progress of the magma. In addition, with approach to this depth the magma, still saturated with water (it will contain ~ 0.5-0.7 wt.% water), will be degassing through rapid vesiculation and crystal growth and/or glass formation. Degassing will be by rapid gas escape through tiny cracks throughout the basalt. If vesiculation occurs, it would cause a significant increase in magma volume that will go to further plugging of the drift, greatly decreasing the penetration distance. If the drift is sealed

by plan or accident, there is also the possible effect of the inflow being resisted by progressive compression of the air by the advancing flow. Lejeune et al. (2002) show that this could be a major effect in retarding the inflow, regardless of fluid viscosity. Throughout this process, the driving pressure will change in concert with the motion of the magma itself. To estimate properly the penetration distance of magma flowing into the drift, each of these effects and factors must be simultaneously taken into account. With due care and insight into the physics of magmatic processes and consideration of the full eruptive scenario a meaningful and useful model can certainly be developed as outlined herein, but it has not been so far attempted.

4. Discussion

Explosivity vs Mobility: There is an important fundamental difference in the dynamic behavior of 'dry' (e.g., <~0.5 wt.% dissolved (primarily H_2O) gas) and 'wet' basaltic magma. Dry Hawaiian-type magma erupts at near-liquidus temperatures, is of low explosivity, but due to low viscosity is highly mobile; its danger is its mobility. Wet basaltic magma, on the other hand, also approaches the surface at near-liquidus temperatures, but because this liquidus is at a much lower temperature, *commonly at or below the 1-atm solidus*, it arrives at the surface near its solidus. That is, any ensuing lava spontaneously quenches, in essence, to a high temperature glass riddled with crystallites that continue to grow from the high temperature glass. Wet basaltic magma is thus initially highly explosive, due to de-volatilization and massive vesiculation and fragmentation, but the eventual lavas are sluggish and immobile. The danger is the high explosivity and not lava mobility.

In all modeling of the flow of magma into the Yucca Mountain Repository, insight into the nature of the magma likely to be involved has been gathered from the nearby alkali basalt cinder cones. The almost universal tendency in prior modeling has been to use a volatile-rich basaltic magma as the characteristic magma involved in all interactions with the Repository. This is the deep pre-eruptive magma containing 2-4 wt.% water with a viscosity of 5-50 Pa s, making it (unrealistically) both highly explosive and highly mobile. Typical calculated flow velocities are 10-100 m/s (i.e., 22-220 mph). This lava flows a distance of 1 km in 10-100 seconds. A similar flow, assuming enough magma were available, would reach the outskirts of Las Vegas (150 km) in as short a time as 40 minutes. There is nothing in the character of the erupted lavas in the region of Yucca Mountain that would suggest any behavior of this nature. On the contrary, the flows from the cinder cones scattered throughout the proximal region are of exceedingly limited spatial extent (~1 km in radius). This limited extent is also not merely due to the slope of the terrain nor to the limited volume of these eruptions, although this is certainly partly the reason. For if the Lathrop Wells governing viscosity is reduced to 10 Pa s, keeping the volume at 0.03 km^3, the flow would have traveled 5 km in about 2 days instead of taking a month or more to go such a distance. This inference is reinforced by the rheology of all magmatic silicate glasses, which, almost regardless of composition, fall in a surprisingly narrow range (e.g., ~$10^{11.5}$ to 10^{12} Pa s at about 750°C).

Altogether, the P-T eruptive history, the glass rheology, and the flow history of lava each suggest that, should alkali basalt of the general nature of that erupted at nearby Lathrop Wells intersect and enter the Repository drifts, the extent of flow will be exceedingly limited. Depending on the exact nature of the flow, the distance of penetration may perhaps be no more than about 10 meters, certainly less than 100 m. Even based simply on the nature of the flows at Crater Flat, the lava would be blocky and sluggish and advancement would be difficult in a small

cylindrical Repository drift, especially one filled with waste packages. It certainly would not be a simple case of a viscous, non-solidifying fluid flowing along a pipe. And, contrary to the analysis of Woods et al. (2002), there is no chance that the lava would undergo any form of wholesale thermal convection whatsoever (Marsh, 1989; Brandeis and Marsh, 1989 and 1990; Hort et al., 1999), nor is it likely that conditions would permit development of a dog-leg eruptive scenario.

Quenching: All magma on Earth's surface is undergoing crystallization and will quench on all that it touches whether it be roads, tress, water, or other rock. It will certainly quench on the metal jacketing the containers of nuclear waste. A 10 cm thick rind of glassy alkali basalt will encase the waste package (and coat the drift walls) in about a minute and will continue to grow with time. Once formed, there is also the question of the possible later reheating or 'burning back' of the quenched rind. Because of the anticipated nature of the magma, in terms of temperature and duration and style of eruption, this is highly unlikely.

The high viscosity of the magma ensures that any flow will be sluggish and cooling will be by conduction with or without latent heat depending on the extent of crystallization and glass formation. When magma touches a cooler surface the temperature at the interface or contact becomes approximately the average of the two initial temperatures. This holds even if the magma is flowing as lava. That is, the interface temperature $T = 0.5\ (T_1+T_2)$, where T_1 and T_2 are the initial temperatures of the magma and object contacted. This is the well-known result found earlier (e.g., Jaeger, 1968; Turcotte and Schubert, 1982; Marsh, 1989). Strictly speaking, this result only holds if there is no latent heat of crystallization involved, which would hold for only glass formation, and if latent heat is included to cover full crystallization the constant changes to 0.65. For magma at 1050°C and a waste package at 200°C, the interface temperature will be about 650°C, which is far below the magma solidus temperature, promoting massive quenching. In the cooling of two juxtaposed planar sheets of material, this temperature does not change until the cooling front has reached the center of the hotter body and then this contact temperature slowly decreases with time. This condition of planar sheets is not met for magma against a cylindrical waste package in a repository drift, but it is approximately met for a rind that is thin relative to the radius of curvature of the waste package. An estimate of the actual magma temperature necessary to reverse cooling can be determined by finding the conditions when cooling is arrested, which can be determined by employing the well known Schwarz solution (Carslaw and Jaeger, 1959). The most general result shows that for no quenching, the sum given above (i.e., T_1+T_2) must be twice the melting temperature of the wall material. If the quenched rind is taken as the wall material at a temperature of 650°C, which at the very least has a 'melting' temperature of 1050°C, then the magma temperature must be about 2100 – 650 = 1450 °C, which is well beyond the eruption temperature of any known terrestrial basaltic magmas. Once formed, under these conditions the quench rinds are an irreversible feature, reflecting the fundamental feature of all subaerial magma in irreversibly cooling to ambient conditions.

We hasten to add, that there are clearly conditions predicted by this analysis where quench rinds or chilled margins can be stalled or even burned back, and these reflect magma flow in already hot (i.e., previously heated) wall rock. Lava tubes that form on some volcanoes, for example, like at Kilauea and Etna, are a reflection of the prolonged volumetric output of the system. They form within a package of fresh lava at near magmatic temperatures where thick lateral thermal boundary layers insulate the flow. Using the above formulation, quenching can be forestalled if initially $T_1 = T_2$, which means that the walls are of the same temperature as the magma and this is the approximate condition prevailing in lava tubes, but not in the repository

drift. Features of the nature of lava tubes could not form in cold drifts as small as proposed for the repository.

Earlier History: Prior to the arrival of lava the leading region of the ascending dike will be laden with gas and tephra. That is, should an ascending dike of water-saturated basaltic magma encounter the repository, the already rapidly quenching magma will undergo even stronger exsolution-induced quenching. Instead of fluid magma entering the drift and flowing along to eventually fill it, as in filling a bathtub, a small cinder cone will begin developing at the point of intersection. (The earliest dynamic phase of this interaction is treated by Dartevelle and Valentine (2005).) Cinders will avalanche into the drift, rapidly piling up and plugging the drift; the fragmental material will not flow far, especially given the presence of waste packages and other components of the engineered barriers. The insulating effect of the close wall rock will minimize air-fall and radiant heat loss, allowing the pile of cinders and tephra to tack or partially anneal together to form a mass of some strength. Magma will continue to quench on this mass of cinders and tephra. This process will form a plug in the drift, sealing the point of intersection, which will either force the magma to continue upward to erupt on the surface or simply seal off the dike locally, redirecting the flow to other portions of the dike that have already reached the surface (e.g., Gaffney and Damjanac, 2006).

The initial 'hole' in the wall of the ascending dike causes a local depressurization producing a perturbation in the pressure field driving the dike upward. This pressure perturbation will travel outward into the dike, informing, in effect, the broader flow of the presence of this vent. But because the rent into the repository is small relative to the surface area of the dike (for a typical dike length of 1 km, this ratio is $\sim 10^{-5}$), this perturbation is relatively small and will not travel far in the thin (~1-10 m) dike before (<~1 s) the rapidly ascending dike (~km/s) reaches the nearby surface, short-circuiting the flow from the Repository drift to the surface.

The formation of a plug at the point of magma entry into the repository will also allow pressures on the dike side of the plug to return to the initial pressure. The initial magma pressure within a basaltic dike at Yucca Mountain may be in the range of 4.5 MPa to 8.0 MPa (i.e., initially ~1 MPa larger than the horizontal far-field stress at repository depth) (Bechtel-SAIC, 2004). The initial magma pressure can also be approximated, as discussed earlier, by the lithostatic pressure at repository depth (i.e., ~7 MPa at 300 m, given a mean tuff density of <2400 kg m^{-3}). Although in light of the earlier evaluation of possible pressure gradients in the arriving magma this is clearly an extreme, it is useful for comparison to the strength of a tephra plug.

Schultz (1995) has measured the strength of the Cohassett basalt flow of the Columbia River Basalt Group. Intact basalt at 20°C and at < 9 MPa confining pressure has a compressive strength of 266 ± 98 MPa, a cohesive strength of 66 MPa, and a tensile strength of ~14 ± 3 MPa. Basalt has a shear strength in the range of 20-60 MPa. A welded tephra plug need only achieve ~3% of the compressive strength or 1/3 to 1/8 of the shear strength of intact basalt to withstand the full pressure that could be exerted by magma in an adjacent dike. A compressive strength of 7 MPa, for example, is more typical of clay soils than of rocks. Increasing temperature into the melting range, however, significantly reduces the strength of basalt. The strength of partially molten basaltic magma under tension has been estimated from a summary of experimental and observational results by Marsh (2002). At ~50 vol.% crystals, mush strength increases from about 0.03 MPa to about 30 MPa at ~ 100% crystals and about 1000°C. For tensile strengths these estimates decrease by a factor of 10-20 (e.g., Jaeger and Cook, 1979). Although these estimates hold only for massive, intact material, fragmental tephra will tend to tack together,

forming a continuum under these high temperature conditions, and due to slow cooling may undergo limited congealing and flow (e.g., Sumner, 1998).

The tephra plug also could not readily be pushed along the drift by either later higher density tephra or magma. Tephra will tend to tack to the tunnel walls and also be obstructed by waste packages aligned in series. More important, perhaps, is that tephra being fragmental material at maximum packing will, like any particulate medium at near maximum packing, dilate upon shear and form a stiff plug (e.g., Marsh, 1981). The net effect is that, after a brief local perturbation, magma is most likely to continue flowing to the surface in the original dike. The area of the drift affected by the invading magma may be minimal, and the number of waste packages affected may therefore be very limited.

After the initial tephra phase, is it possible that magma would flow through the interstices of a welded tephra plug? Little flow would occur because of the high viscosity of the degassing magma, which would move as a high temperature glass.

The work by Nicholis and Rutherford (2004) and Luhr and Housh (2002) indicates water contents of 1.9% to 4.6% for melt inclusions from two Pleistocene vents in Crater Flat (Lathrop Wells and Red Cone). Mineral phase assemblages indicate that magmas in Crater Flat erupted at temperatures of <975°C (Little Cones) and ~1000-1010°C (Lathrop Wells). The water contents and implied pyroclastic activity are consistent with the observed tephra cones in Crater Flat and provide evidence that the expected result of a vent or dike intersection with a repository would be the rapid formation of tephra plugs in drifts. This scenario is *most likely* for Yucca Mountain because repository drifts would be constructed at elevations ~200 m *lower* than the basin floor west of the mountain. Therefore, rising dikes or conduits would encounter the repository drifts before reaching the surface, when volatile contents could be expected to still be elevated.

Finally, as tempting as it may be to consider lava tubes as analogs to the hypothetical case of magma entering tunnels at Yucca Mountain, lava tubes form in high volume, high temperature, low viscosity, volatile-poor magmatic systems, like Hawaii. They are generally not found in small volume, mono-genetic, volatile-rich magmatic systems. Moreover, the general applicability of insights gained from high temperature, highly mobile lavas to the anticipated style of magmatism at Yucca Mountain is questionable.

5. Summary

In striving to anticipate and analyze the effects of magma intersecting and entering the proposed Yucca Mountain Nuclear Repository, there has been a strong tendency to assume magma properties and characteristics from an assortment of magmatic environments. Assuming the magma to be both highly explosive *and* highly mobile is inconsistent with the inferred nature of the alkali basalt magma historically erupted in this region. The most likely magma, considering the nearby Lathrop Wells alkali basalt, will be explosive, due to containing 2-4 wt.% water, but this will also make the associated lava sluggish and immobile. This is due to its inherently low temperature, which is near or below the 1-atm solidus, as it approaches the surface. The ensuing lava has the apparent rheological properties of a high temperature, highly viscous glass, which is consistent with the spatially limited flow fields emitted by cinder cones of the type of Lathrop Wells. This severely limits the distance of penetration of this lava into Repository drifts to perhaps 10 m, which limits the number of waste packages potentially affected by the lava. Lava encountering waste packages will quickly (minutes) form permanent quench rinds of significant thickness (>10 cm), which will further insulate waste against

remobilization. To gain some physical perspective for the relationship between a drift and an actual lava flow, Figure 19 shows a scale drawing of a drift superimposed on the lava flow front at Lathrop Wells. In this perspective it can be appreciated how difficult it will be for lava of this nature to penetrate a typical drift. The blocks characteristic of flows of this nature are of a scale commensurate with the scale of the proposed repository drifts. And even though there could be less rigid, highly viscous magma interspersed among these blocks, the overall ability of the flow to move is severely limited by this basic nature.

Figure 19. ----------***near here***

These considerations illustrate the basic nature of the ascent and solidification processes that present themselves when an integrated system of a specific magma type and composition interacts with waste packages. These calculations and results illustrate the importance of treating these magmatic processes as comprehensively and realistically as possible. More detailed calculations could be done within this framework to flesh out further and establish the nature of these and other processes involving solidification and magma flow. However, at this point, based on our results, it is unlikely that a repository at Yucca Mountain would be seriously compromised by future igneous processes of the kind anticipated herein. The number of waste packages directly affected by magmatic intrusion is expected to be small.

Acknowledgments. This study was undertaken as part of a larger study by the late Advisory Committee for Nuclear Waste and Materials on the technical basis for decision making for the proposed repository at Yucca Mountain (ACNW&M; Hinze et al., 2008a; b). The subjects considered in the present study, along with many others, are considered in this broader work. Views expressed are the authors' and do not necessarily represent those of the U.S. NRC. We appreciate help with some of the phase equilibria calculations by Kaustubh Patwardhan and some of the analytical approaches by Thomas Haine. Thoughtful reviews by Dennis Geist and anonymous others are much appreciated. Lengthy and stimulating conversations with William Hinze and Ruth Weiner contributed significantly to sharpening our effort. The essence of this material has been presented by the senior author in lectures at Pomona College, San Francisco State University, Whitman College, and at the University of Akron. Research on magmatic processes in general by BDM has long been supported by the National Science Foundation, most recently by NSF Grant OPP 0440718 to the Johns Hopkins University.

Appendix I

Appendix I: Physical Properties of Basaltic Magma (rock) and Waste Package Materials

Parameter	Value
Emplacement drift diameter	5.5 m
Drift length[1]	650-800 m
Commercial spent nuclear fuel waste packages	
Alloy 22 outer barrier	2 cm thick
316 NG stainless steel inner barrier	5 cm thick
WP outer diameter[2]	
21-PWR	1.6 m
44-BWR	1.7 m
WP outer length[2]	
21-PWR	5.2 m
44 BWR	5.2 m
WP mass (loaded)[2]	
21-PWR	42,300 kg
44-BWR	42,500 kg
WP volume	
21-PWR	10.4 m^3
44-BWR	11.8 m^3
WP density	
21-PWR	4067 kg/m^3
44-BWR	3602 kg/m^3
WP thermal conductivity	
Alloy 22[3]	27.5 W/m-K @ 1100°C
	16.4 W/m-K @ 500°C
Alloy 22[4]	19.5 W/m-K @ 500°C
316 NG stainless steel[4]	21.1 W/m-K @ 510°C
Spent nuclear fuel assembly[4]	1.39 W/m-K @ 400°C
WP specific heat	
Alloy 22[3]	381 J/kg-°C
Alloy 22[4]	485 J/kg-K @ 500°C
316 NG stainless steel[4]	566 J/kg-K @ 510°C
Spent nuclear fuel assembly[4]	274 J/kg-K
WP thermal diffusivity	
Alloy 22	4.5 $x10^{-6}$ m^2/s @ 500°C (calculated value)

316 NG stainless steel[4,5]	4.67 x10^{-6} m^2/s @ 510°C
WP melting range	
Alloy 22[3]	1351-1387°C
316 NG stainless steel[6]	1375-1400°C (typical for grades 316 and 316L)
Metal density	
Alloy 22[4,5]	8690 kg/m^3
316 NG stainless steel[4,5]	7980 kg/m^3

Magma Properties[7]

Magma density	2500 kg/m^3
Magma thermal conductivity	1.818 W/m-°C
Magma specific heat	900 J/kg-°C
Magma thermal diffusivity	0.8 x$10^{-6}$$m^2$/s

---

[1]Harrington, P. (2007). Status of Yucca Mountain Repository Design. Presentation to the Advisory Committee on Nuclear Waste and Materials, US NRC, Rockville, MD, November 14, 2007.

[2]U.S. Department of Energy (2002). Yucca Mountain Science and Engineering Report, Technical Information Supporting Site Recommendation Consideration, Rev. 1, DOE/RW-0539-1.

[3]Special Metals Corporation (2006). Technical Bulletin on properties of Inconel® Alloy 22, Publication Number SMC-049, Available online at: http://www.specialmetals.com/documents/Inconel%20alloy%2022.pdf.

[4]Faucher, F. P. (2000). Thermal response of the 21-PWR Waste Package to a Fire Accident, CAL-UDC-TH-00002 Rev 0, Prepared for U.S. Dept. of Energy, Office of Civilian Radioactive Waste Management, 39 p.

[5]Smotrel, J. R. (2001). Thermal response of the 44-BWR Waste Package to a Hypothetical Fire Accident, CAL-UDC-TH-000004 Rev 0, Prepared for U.S. Dept. of Energy, Office of Civilian Radioactive Waste Management, 47 p.

[6]British Stainless Steel Association (2007). Melting temperature ranges for stainless steels, Fact Sheet available online at: http://www.bssa.org.uk/topics.php?article=103.

[7]Spera, F.J. (2000). Physical properties of magma. Encyclopedia of volcanoes. Academic Press, N.Y., p.171-190.

References

Batchelor, G.K, 1967. An Introduction to Fluid Mechanics. Cambridge Univ. Press, 615 pp.

BSC (Bechtel- SAIC Co.), 2001. FY01 Supplemental Science and Performance Analyses, Vol. 1: Scientific bases and analyses, Rept. Prepared for U.S. Dept. of Energy, TDR-MGR-MD-000007 REV 00, Las Vegas, NV.

Bechtel-SAIC, 2004. Dike/Drift Interactions, Rept. Prepared for US Dept. of Energy, MDL-MGR-GS-000005 REV 01.

Behrens, R.A., Crochet, M.J., Denson, C.A., Metzner, A.B., 1987. Transient free-surface flows: Motion of a fluid advancing in a tube. AIChE Journal 33: 1178-1186.

Bejan, A., 1984. Convective heat transfer. Wiley-Interscience, 477 pp.

Blundy, J., Cashman, K.V., Humphreys, M., 2006, Magma heating by decompression-driven crystallization beneath andesitic volcanoes. Nature 443, 76-80.

Brandeis, G. and Marsh, B.D., 1989. The convective liquidus in a solidifying magma chamber: A fluid dynamical investigation. Nature 339: 613-616.

Brandeis, G., Marsh, B.D., 1990. Transient magmatic convection prolonged by solidification. Geophys. Res. Lett. 17: 1125-1128.

Bruce, P.M. and Huppert, H.E., 1990. Solidification and melting along dykes by the laminar flow of basaltic magma. In: Ryan, M.P. (ed.) Magma transport and storage. J. Wiley and Sons, N.Y., 87-101.

Coleman, N.M., Marsh, B.D., Abramson, L.R., 2004. Testing claims about volcanic disruption of a potential geologic repository at Yucca Mt., NV. Geophys. Res. Lett., doi:10.1029/2004GL021032.

Connor, C.B., Stamatakos, J.A., Ferrill, D.A., Hill, B.E., 1998. Technical Comment on "Detecting Strain in the Yucca Mountain Area, Nevada," by Wernicke et al. [1998]; Science 282: 1007b.

Connor, C.B., Stamatakos, J., Ferrill, D., Hill, B., Ofoegbu, G., Conway, F., Sagar, B., Trapp, J., 2004. Geologic factors controlling patterns of small-volume basaltic volcanism: Application to a volcanic hazards assessment at Yucca Mountain, Nevada. J. Geophys. Res. 105: 417-432.

CRWMS M&O, 2000. Waste Package Degradation Process Model Report, TDR-WIS-MD-000002 REV 00 ICN 01, Prepared for: U.S. Department of Energy by TRW Environmental Safety Systems Inc., Las Vegas, Nevada.

Dartevelle, S., Valentine, G.A., 2005. Early-time multiphase interactions between basaltic magma and underground openings at the proposed Yucca Mountain radioactive waste repository, Geophys. Res. Lett., doi:1029/2005GL0241172.

Del Marmol, M., 1989. The petrology and geochemistry of Merapi volcano, central Java, Indonesia. Ph.D. Dissertation, Johns Hopkins University, Baltimore, MD, 384 pp.

Detournay, E., Mastin, L.G., Anthony, J.R., Pearson, A., Rubin, M., Spera, F.J., 2003. Final Report of the [Yucca Mountain] Igneous Consequences Peer Review Panel, 86 pp.

DOE (US Dept. of Energy), 2003. Technical Basis Document No. 13: Volcanic Events. Report by Bechtel SAIC Company, LLC, for US DOE, WWW page, http://www.ocrwm.doe.gov/documents/38453_tbd/index.htm.

DOE (US Dept. of Energy), 2004. Dike/Drift Interactions. Document 20041124.0002, Report by Bechtel SAIC Company, LLC, for US DOE, 416 pp.

DOE, 2008. Yucca Mountain Repository License Application - Safety Analysis Report. U.S. Dept. of Energy, Office of Civilian Radioactive Waste Management, DOE/RW-0573, Rev. 0, June 2008.

Emeleus, C.H., Bell, B.R., 2005. The Paleogene volcanic districts of Scotland (4th ed.). British Geological Survey, Nottingham, United Kingdom, 212 pp.

EPRI (Electric Power Research Institute), 2004. Potential igneous processes relevant to the Yucca Mountain repository: Extrusive-release scenario, Analysis and Implications. EPRI Tech. Rept. 1008169.

EPRI (Electric Power Research Institute), 2005. Program on Technology Innovation: Potential igneous processes relevant to the Yucca Mountain repository: Intrusive-release scenario. EPRI Tech. Rept. 1011165.

Fewell, M.E., Hardee, H.C., Montoya, C., 1975. Design of a molten-lava, single tube boiler experiment. SAND75-0080, Sandia National Laboratories, Albuquerque, NM.

Fink, J.H., Griffiths, R.W., 1998. Morphology, eruption rate and rheology of lava domes: Insights from laboratory models. J. Geophys. Res. 103 (B1): 527-545.

Frigaard, I.A., Crawshaw, J.P., 1999. Preventing buoyancy-driven flows of two Bingham fluids in a closed pipe-Fluid rheology design for oilfield plug cementing. Jour. Eng. Mathematics 36: 327-348.

Gaffney, E.S., Damjanac, B., 2006. Localization of volcanic activity: Topographic effects on dike propagation, eruption and conduit formation. Geophys. Res. Lett. 33: L14313, doi:10.1029/2006GL026852.

Geomatrix and TRW, 1996. Probabilistic volcanic hazard analysis for Yucca Mountain, NV, prepared for U.S. Dept. of Energy by Geomatrix Consultants, Inc. and TRW, Rep. BA0000000-1717-2200-00082, Rev. 0, San Francisco, CA.

Ghiorso, M., Sack, R., 1995. Chemical mass transfer in magmatic processes IV. A revised and internally consistent thermodynamic model for the interpolation and extrapolation of liquid-solid equilibria in magmatic systems at elevated temperatures and pressures. Contrib. Min. Pet., 119, 197-212.

Griffiths, R.W., 2000. The dynamics of lava flows. Annu. Rev. Fluid Mech. 32: 477-518.

Hammer, J. E., Cashman, K.V., and Voight, B., 2000. Magmatic processes revealed by textural and compositional trends in Merapi dome lavas. Journal of Volcanology and Geothermal Research 100: 165-192.

Hardee, H.C., 1975. Convective heat extraction from molten magma. J. Volcanol. Geotherm. Res. 10: 175-193.

Hardee, H.C., Fewell, M.E., 1975. Molten lava/single tube boiler experiment. Sandia National Laboratories, Albuquerque, NM, SAND75-0069.

Harrington, P., 2007. Status of Yucca Mountain repository design. Presentation to the Advisory Committee on Nuclear Waste and Materials, US NRC, Rockville, MD, November 14, 2007.

Harris, D.M., 1977. Ascent and crystallization of albite and granitic melts saturated with water. Jour. Geol. 85: 451-459.

Heizler, M.T., Perry, F.V., Crowe, B.M., Peters, L., Appelt, R., 1999. The age of Lathrop Wells volcanic center: An $^{40}Ar/^{39}Ar$ dating investigation. J. Geophys. Res. 104 (B1): 767-804.

Hinze, W.J., Marsh, B.D., Weiner, R., Coleman, N.M., 2008a. Igneous activity at Yucca Mountain. Eos, Vol. 89, No. 4 (22 January 2008), 29-30.

Hinze, W.J., Marsh, B.D., Weiner, R., Coleman, N.M., 2008b. Evaluating Igneous activity at Yucca Mountain – Technical Basis for Decisionmaking. NUREG-1890, U.S. Nuclear Regulatory Commission, Washington, DC, 255 pp.

Hon, K., Kauahikaua, J., Denlinger, J., Mackay, K., 1994. Emplacement and inflation of pahoehoe sheet flows: Observations and measurements of active lava flows on Kilauea Volcano, Hawaii. Geol. Soc. Am. Bull. 106: 351-370.

Hort, M., Marsh, B.D., Resmini, R. G., Smith, M. K., 1999. Convection and crystallization in a liquid cooled from above: An experimental and theoretical study. Jour. Petrology 40: 1271-1300.

Huppert, H.E., 1982. Flow and instability of a viscous current down a slope. Nature 300: 427-429.

Huppert, H.E., Shepherd, J.B., Sigurdsson, H., Sparks, S., 1982. On lava dome growth, with application to the 1979 Lava extrusion of the Soufriere of St. Vincent. J. Volcanol. Geotherm. Res. 14: 199-222.

Ibarra, L., Wilt, T., Ofoegbu, G., Kazban, R., Ferrante, F., Chowdhury, A.H., 2007. Drip Shield-Waste Package Mechanical Interaction. Progress Report, Center for Nuclear Waste Regulatory Analyses, San Antonio, Texas.

Jaeger, J.C., 1968. Cooling and solidification of igneous rocks. in H. H. Hess and A. Poldervardt (eds), Basalts: the Poldervaart treatise on rocks of basaltic composition, vol. 2, 503-536, Interscience.

Jaeger, J.C., Cook, N. G. W., 1979. Fundamentals of rock mechanics. Chapman and Hall (London), 593 pp.

Keszthelyi, L., 1995. A preliminary thermal budget for lava tubes on the Earth and planets. J. Geophys. Res. 100: 20,411-20,420.

Koli, V.G., Ogadhoh, S.O., Abel, S.M., Gadala-Maria, F., Papathanasiou, T.D., 2002. Particle motion in the fountain flow regime during filling of a tube with a viscoelastic fluid. Polymer Engineering and Science 42: 403-412.

Lejeune, A.M., Woods, A.W., Sparks, R.S.J., Hill, B.E., Connor, C.B., 2002. "The decompression of volatile-poor basaltic magma from a dike into a horizontal subsurface tunnel," NRC Accession No. ML033640075 (available online at http://www.lsnnet.gov/), 38 pp.

Lescinsky, D.T., Merle, O., 2005. Extensional and compressional strain in lava flows and the formation of fractures in surface crust. In: Manga, M. and G. Ventura (eds.), Geol. Soc. Am. Special Paper 396: 163-179.

Lore, J., Gao, H., Aydin, A., 2000. Viscoelastic thermal stress in cooling basalt flows, J. Geophys. Res. 105: 23,695–23,709.

Luhr, J.F., Housh, T.B., 2002. Melt volatile contents in basalts from Lathrop Wells and Red Cone, Yucca Mountain Region (SW Nevada): Insights from glass inclusions, Eos. Trans. AGU, 83(47), Fall Meet. Suppl., Abstract V22A-1221.

Manas-Zloczower, I., Blake, J.W., Macosko, C.W., 1987. Space-time distribution in a filling mold. Polymer Science and Engineering 27: 1229-1235.

Manley, C.R., 1992. Extended cooling and viscous flow of large, hot rhyolite lavas: Implications of numerical modeling results. Jour. Volcanology and Geothermal Research 53: 27-56.

Mastin, L.G., Ghiorso, M.S., 2001. Adiabatic temperature changes on magma–gas mixtures during ascent and eruption. Contr. Min. Pet. 141: 307-321.

Mastin, L.G., 2005. The controlling effect of viscous dissipation on magma flow in silicic conduits. Jour. Volcanol. Geotherm. Res. 143: 17-28.

Marsh, B.D., 1978. On the cooling of ascending andesitic magma. Philosophical Transactions of the Royal Society of London 288: 611-625.

Marsh, B.D., 1981. On the crystallinity, probability of occurrence, and rheology of lava and magma, Contr. Min. Pet. 78: 85-98.

Marsh, B.D., 1984. Mechanics and energetics of magma formation and ascension. In J. Boyd (ed.) Explosive Volcanism: Inception, Evolution, and Hazards, National Academy Press, 67-83.

Marsh, B.D., 1989. Convective style and vigour in magma chambers. Jour. Petrology 30: 479-530.

Marsh, B.D., 1990. Amak, Aleutian Islands, Alaska; Atka, Central Aleutian Islands; Buldir, Western Aleutian Islands; Gareloi, Western Aleutian Islands; Moffett and Adagdak, Central Aleutian Islands; and Tanaga, Central Aleutian Islands. In: C.A. Wood, J. Kienle (Editors), Volcanoes of North America United States and Canada, Cambridge University Press, Cambridge, UK, 354 pp.

Marsh, B.D., 1996. Solidification fronts and magmatic evolution, Mineralogical Magazine 60: 5-40.

Marsh, B.D., 1998. On the interpretation of crystal size distributions in magmatic systems, J. Petrology 39, 553-599.

Marsh, B.D., 2000. Magma chambers, Encyclopedia of Volcanoes. Academic Press, 191-206.

Marsh, B.D., 2002. On bimodal differentiation by solidification front instability in basaltic magmas, Part I: Basic mechanics. Geochim. et Cosmochim. Acta, 66: 2211-2229.

Marsh, B.D., 2004. A magmatic mush column rosetta stone: The McMurdo Dry Valleys of Antarctica. EOS Trans. Amer. Geophys. Union, 85, no.47, 497-502.

Marsh, B.D., 2007, Magmatism, magma, and magma chambers. *In* Treatise on Geophysics: The Crust. Chapter 6, p. 276-333. Elsevier.

Mohanty, S., et al., System-level performance assessment of the proposed repository at Yucca Mountain using the TPA version 4.1 code, NRC accession no. ML041350316, 2004.

Morris, S.J.S., 1982. The effects of a strongly temperature-dependent viscosity on slow flow past a hot sphere. Jour. Fluid Mech. 124: 1-26.

Nairn, I.A., 1976. Atmospheric shock waves and condensation clouds from Nguaruhoe explosive eruptions. Nature 259: 190-192.

Navon, O. and V. Lyakhovsky, Vesiculation processes in silicic magmas. In: Gilbert, J.S. and Sparks, R.S.J. (eds.), The physics of explosive volcanic eruptions. Geol. Soc. London, Spec. Pubs. 145: 27-50.

Nicholis, M.G. and Rutherford, M.J., 2004. Experimental Constraints on Magma Ascent Rate for the Crater Flat Volcanic Zone Hawaiite. Geology 32(6): 489–492.

NRC, 2007. Total-system Performance Assessment (TPA) Version 5.1 Module Descriptions and User Guide. NRC Accession No. ML072710060, Prepared for NRC by Center for Nuclear Waste Regulatory Analyses, San Antonio, TX, 704 pp.

Papale, P., 1997. Modeling of the solubility of a one-component H_2O or CO_2 fluid in silicate melts. Contr. Min. Pet.126: 237-251.

Ofoegbu, G., Fedors, R., Grossman, C., Hsiung, S., Ibarra, L., Manepally, C., Myers, J., Nataraja, M., Pensado, O., Smart, K., Wyrick, D., 2007. Summary of Current Understanding of Drift Degradation and Its Effects on Performance at a Potential Yucca Mountain Repository. CNWRA 2006-02. Center for Nuclear Waste Regulatory Analyses, San Antonio, Texas.

Reed, J.W., 1980. Air pressure waves from Mount St. Helens eruptions. EOS Trans. Amer. Geophys. Union 61: 1136.

Rutherford, M.J., Sigurdsson, H., Carey, Davis, A., 1985, The May 18, 1980, eruption of Mount St. Helens 1. Melt composition and experimental phase equilibria. Jour. Geophys. Res. 90, 2929-2947.

Sahagian, D.L., Proussevitch, A.A., 1996. Thermal effects of magma degassing. Jour. Vol. Geother. Res. 74: 19-38.

Savage, J., Svarc, J.L., Prescott, W.H., 2001. Strain accumulation near Yucca Mt., NV, 1993-1998. J. Geophys. Res. 106 (B8): 16,483-16,488.

Schultz, R.A., 1995. Limits on strength and deformation properties of jointed basaltic rock masses, Rock Mech. and Rock Eng. 28: 1–15.

Shaw, H.R., 1969. Rheology of basalt in the melting range. Jour. Petrology 10: 510-535.

Smith, E.I., Keenan, D.L., 2005. Yucca Mountain could face greater volcanic threat. EOS, Trans., Amer. Geophys. Union, 86(35), p. 317 and 321.

SNL (Sandia National Laboratories), 2008. Probabilistic Volcanic Hazard Analysis Update (PVHA-U) for Yucca Mountain, Nevada. TDR-MGR-PO-000001, Rev. 00. Prepared for U.S. Dept. of Energy by Sandia National Laboratories.

Spera, F.J., 2000, Physical properties of magma. In, Sigurdsson, H., Encyclopedia of Volcanoes. Academic Press, N.Y., 171-190.

Spohn, T, 1980. Orogenic volcanism caused by thermal runaways? Geophys. Journal of the Royal Astronom. Soc. 62: 403-419.

Sumner, J.M., 1998, Formation of clastogenic lava flows during fissure eruption and scoria cone collapse: the 1986 eruption of Izu-Oshima Volcano, eastern Japan. Bull. Volcanology, 60, 195-212.

Takahashi, T.J., Griggs, J.D., 1987. Hawaiian Volcanic Features: A Photoglossary. In Decker, R.W., T.L. Wright and P.H. Stauffer, Volcanism in Hawaii, Vol. 2. U.S.G.S. Prof. Paper 1350, U.S. Gov Printing office, 845-902.

Valentine, G.A., Perry, F.V., Krier, D., Keating, G.N., Kelly, R.E., Cogbill, A.H., 2006. Small-volume basaltic volcanoes: Eruptive products and processes, and post eruptive geomorphic evolution in Crater Flat (Pleistocene), southern Nevada. Geol. Soc. Amer. Bull., Nov./Dec. 118: 1313-1330.

Valentine, G.A., Krier, D.J., Perry, F.V., Heiken, G., 2007. Eruptive processes at the Lathrop Wells scoria cone. J. Volcanol. Geotherm. Res. 161: 57-80.

Wernicke, B., Davis, J.L., Bennett, R.A., Elósegui, P., Abolins, M.J., Brady, R.J., House, M.A., Niemi, N.A., Snow, J.K., 1998. Anomalous strain accumulation in the Yucca Mountain Area, Nevada. Science 279: 2096-2100.

Winslow, N., Marsh, B.D., 2007. Liquidus tracking by vigorous convection in ascending magma Abstract V53C-1432, EOS, Trans. Amer. Geophys. Union, Fall meeting, San Francisco.

Woods, A.W., Sparks, S., Bokhove, O., LeJeune, A., Connor, C.B., Hill, B.E., 2002. Modeling magma-drift interaction at the proposed high-level radioactive waste repository at Yucca Mountain, Nevada, USA, Geophys. Res. Lett., doi:10.1029/2002GL014665.

Wright, T.L., Okamura, R.T., 1977. Cooling and crystallization of tholeiitic basalt, 1965 Makaopuhi lava lake, Hawaii, U.S. Geological Survey Professional Paper, 1004, 78 pp.

Wylie J.J., Helfrich K.R., Dade B., Lister J.R., Salzig J.F., 1999, Flow localization in fissure eruptions. Bull Volcanol 60:432–440.

Zieg, M.J., Marsh, B.D., 2005. The Sudbury igneous complex: Viscous emulsion differentiation of a superheated melt sheet. Geol. Soc. Am. Bull. 117: 1427-1450.

Figure Captions

Figure 1. Schematic depiction of the anticipated repository tunnel (drift) containing waste packages within Yucca Mtn.

Figure 2. Anticipated temperatures over a period of time of 100 ka within the repository drift at Yucca Mtn. due to the presence of typical waste packages, where the temperature of the WP and its drip shield is also noted (CRWMS, 2000; BSC, 2001).

Figure 3. Five possible intrusive-extrusive scenarios for magma interaction with waste packages including the so-called 'dog leg' scenario (lowermost).

Figure 4. Upper two diagrams: Variation of crystallinity (left axis) with temperature (bottom axis) for Hawaiian tholeiitic basalt and alkali basalt from Lathrop Wells, Nevada. The lower diagram shows in a schematic sense the possible variations in viscosity for cooling paths involving only crystallization and crystallization and/or glass formation for a dry magma.

Figure 5. Tree casts in Hawaii formed by lava quenching on trees with subsequent combustion of trees, leaving the quenched rind as the flow subsided and thinned (from Takahashi and Griggs, 1987).

Figure 6. The time to grow a quenched rind on a WP as a function of the quenched rind thickness d.

Figure 7. Upright Paleocene conifer caught in a thick basalt flow in Scotland. The distinctive quenched rinds have been noted along with the strong horizontal columnar jointing reflecting the overall effect of quenching and local rapid cooling. Also notice the man for scale. (after Emeleus and Bell, 2005).

Figure 8. Ultramafic mantle nodule xenolith caught in vesicular alkali basalt lava with well-developed quenched rind. Scale at base is in centimeters.

Figure 9. Radial extent of the Lathrop Wells, Nevada lava field as a function of the duration of the flow event for (a) a range of kinematic viscosities and (b) and range of total lava volume for a single value of kinematic viscosity of 10^9 cm^2/sec. The observed flow extent is about 1 km and the volume is about 0.03 km^3.

Figure 10. The viscosity of a radially spreading lava flow when the lava is emitted at a prescribed flux and (a) duration of one or two months and (b) the time to form a radial flow of 500 m for a series of eruptive fluxes.

Figure 11. The flow extent of lava of a given thickness and viscosity moving down a slope inclined at 1° over a period of time up to six months.

Figure 12. Phase diagrams for generic basalt as a function of pressure under Dry and Wet conditions with indications of possible ascent paths along the dry liquidus and also along a

steeper isentropic adiabat. For low initial crystallinity magma ascends from depth along the liquidus due to the rapid dissipation of potential superheat by vigorous thermal convection. The net effect for dry magmas is that they erupt at near liquidus temperatures whereas for wet magmas the ultimate ascent path may be at sub-solidus temperatures.

Figure 13. (a) Phase diagram for Lathrop Wells basalt under Dry and Wet conditions; a possible near surface ascent trajectory is also indicated where the curvature to slightly higher final temperatures is due to volumetric heating from latent heat of crystallization forced by volatile exsolution. (b) An example of near surface magma (Mt. St. Helens dacite) that began its final ascent from subsolidus temperatures and experienced ~60 °C of heating due to plagioclase crystallization (data from Blundy et al. (2006)). Note the dry liquidus and solidus relative to the wet liquidus and solidus.

Figure 14. Change in temperature for water-rich basalt (lower axis) and rhyolite (upper axis) magma ascending from a pressure of 200 MPa under constant entropy (after Mastin and Ghiorso, 2001).

Figure 15. The viscosity of glasses of magmatic compositions measured as a function of strain rate by Webb and Dingwell (1990). The stippled area on the left is the probable range of strain rates for lava extrusion at Lathrop Wells. Notice the small range of viscosities in spite of the large contrast in compositions.

Figure 16. Estimates of the possible governing pressure gradients that may drive the flow of magma into a repository drift as a function of magma viscosity. The horizontal bars bracket the driving pressure as based on various hypothetical physical situations as described in the text. The slanting lines show the similar tradeoff in driving pressure as a function of magma viscosity as constrained by the observed volume of lava found at Lathrop Wells to have erupted from vent radii of 5 to 20 m and at mean flux rates of 1-10 m^3/sec. The independent sets of results overlap in the high viscosity range of~10^8 to 10^9 p and where the driving pressure gradient is ~1 bar/m.

Figure 17. The flow or penetration distance of lava along a repository drift as a function of (a) magma viscosity, for specific values of effect drift diameter and flow duration and (b) as a function of flow duration for specific values of viscosity and effective drift diameter.

Figure 18. The approximate magma penetration distance as a function of the maximum driving pressure exerted over various effective distances (as noted) as functions of (a) magma viscosity and (b) time for an effective drift diameter of 3.5 m. Along the lower axis of (b) is the result if the flow is driven by a pressure gradient similar to that driving a lava flow.

Figure 19. The geometric form of the proposed repository drift containing a waste package superimposed to approximate scale on the lava flow front at nearby Lathrop Wells; note the man for scale. This is the distal end of the lava at a distance of about 1 km from the vent where the flow is thicker. At this point the scale of the larger individual rigid blocks throughout the flow are of the scale of the drift itself.

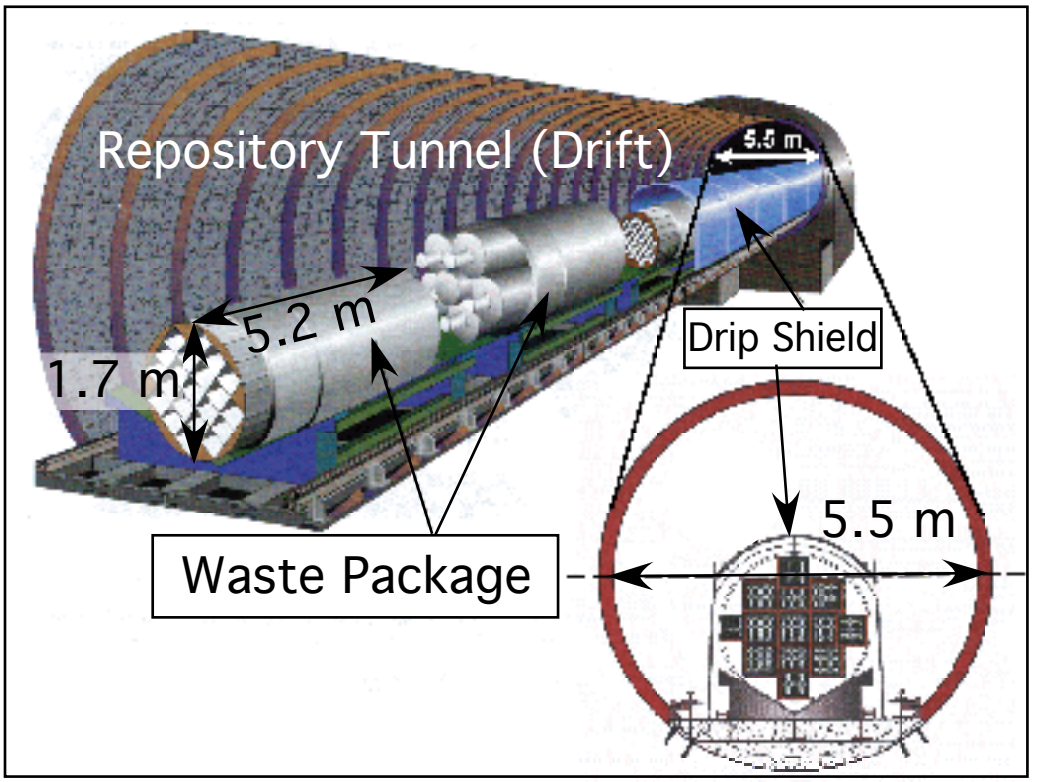
Repository Tunnel (Drift)
5.5 m
5.2 m
1.7 m
Drip Shield
5.5 m
Waste Package

Figure 1

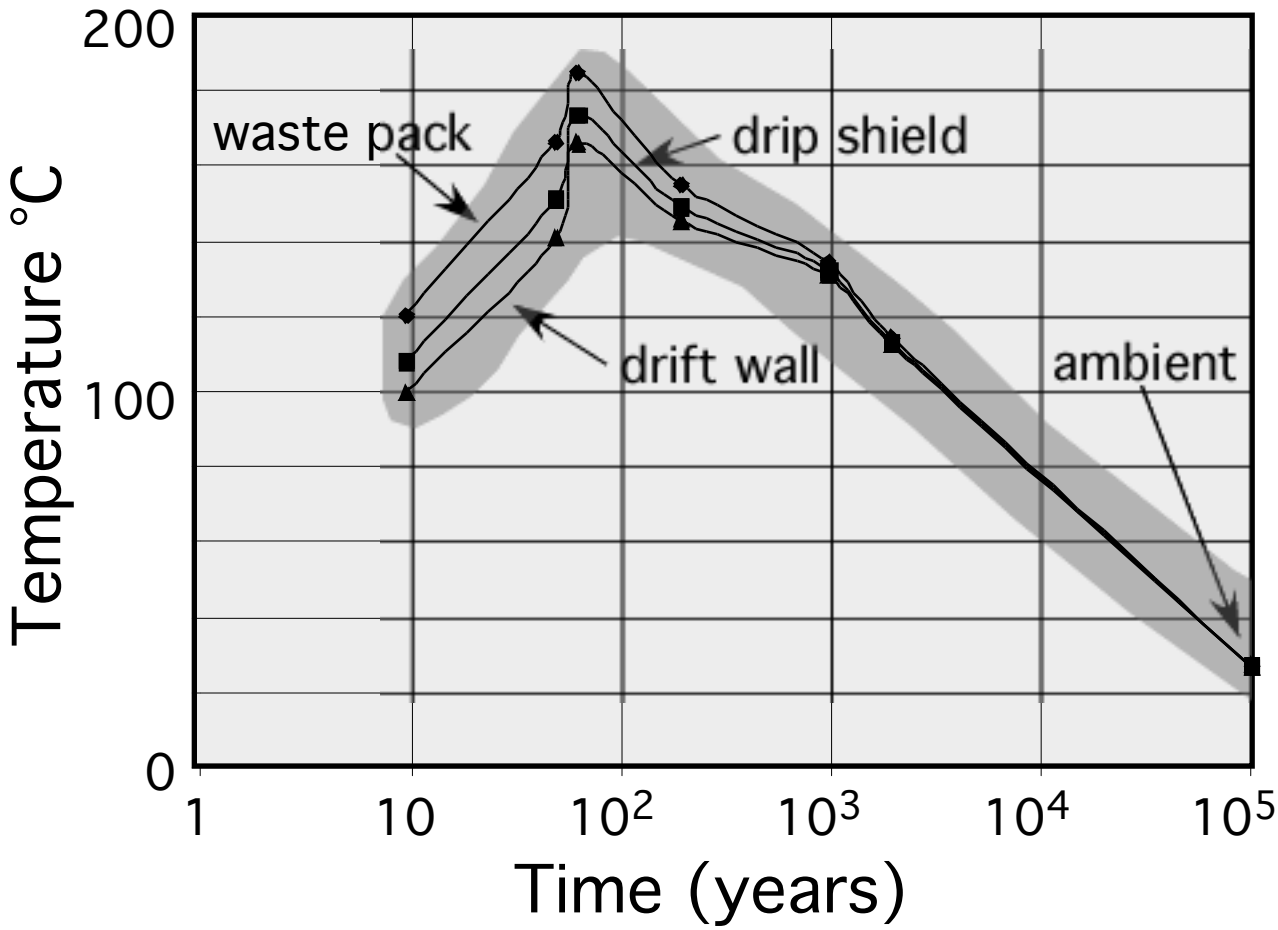
200
100
0
Temperature °C
waste pack
drip shield
drift wall
ambient
1
10
10^2
10^3
10^4
10^5
Time (years)

Figure 2

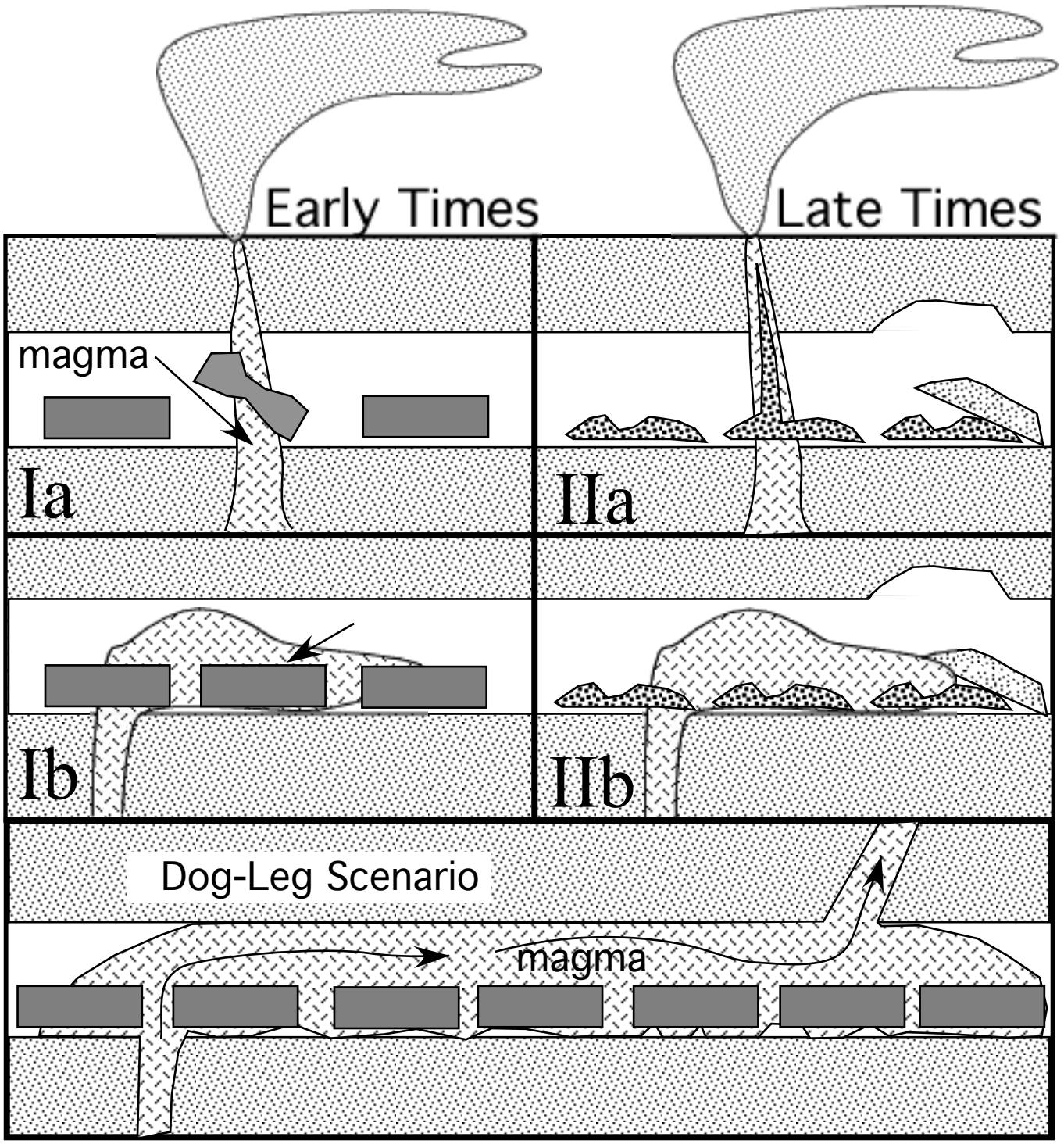
Early Times
Late Times
magma
Ia
IIa
Ib
IIb
Dog-Leg Scenario
magma

Figure 3

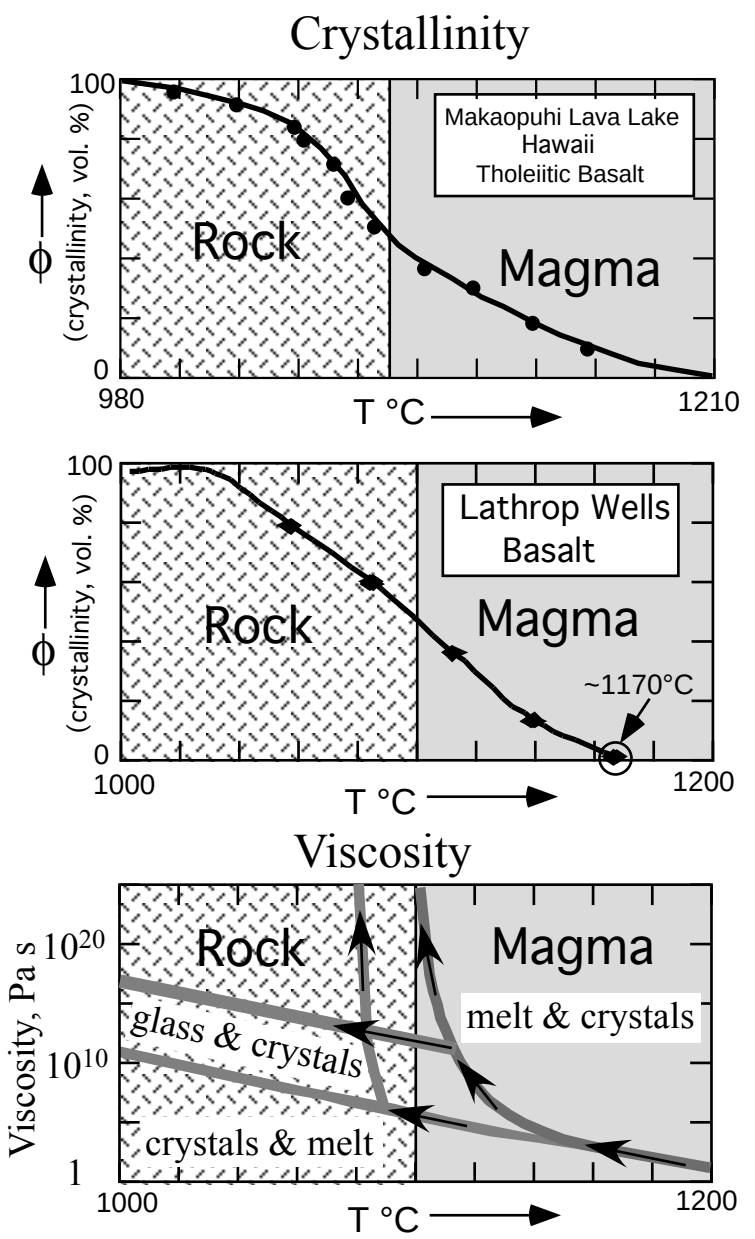
Crystallinity
100
0
ϕ (crystallinity, vol. %)
Makaopuhi Lava Lake
Hawaii
Tholeiitic Basalt
Rock
Magma
980
T °C
1210
100
0
ϕ (crystallinity, vol. %)
Lathrop Wells
Basalt
Rock
Magma
~1170°C
1000
T °C
1200
Viscosity
Viscosity, Pa s
10^{20}
10^{10}
1
Rock
Magma
melt & crystals
glass & crystals
crystals & melt
1000
T °C
1200

Figure 4

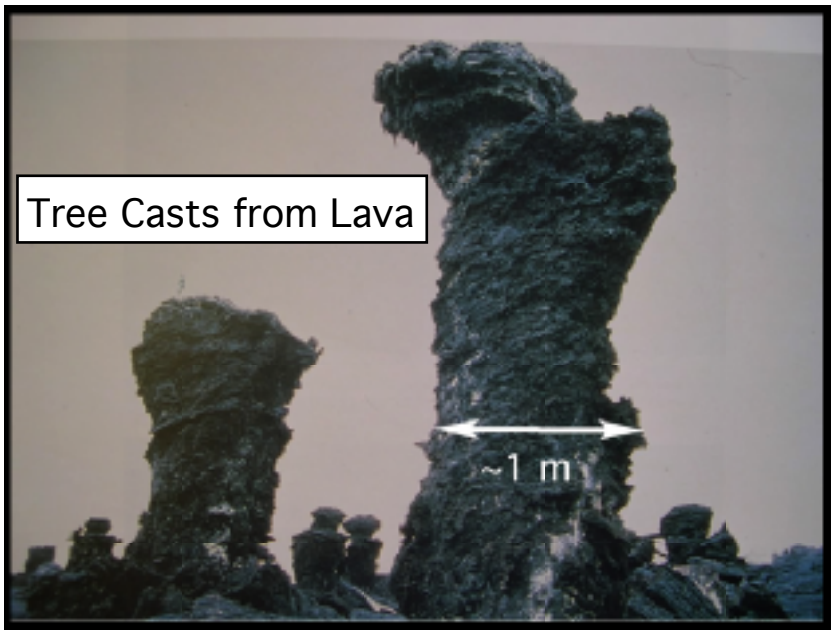

Figure 5

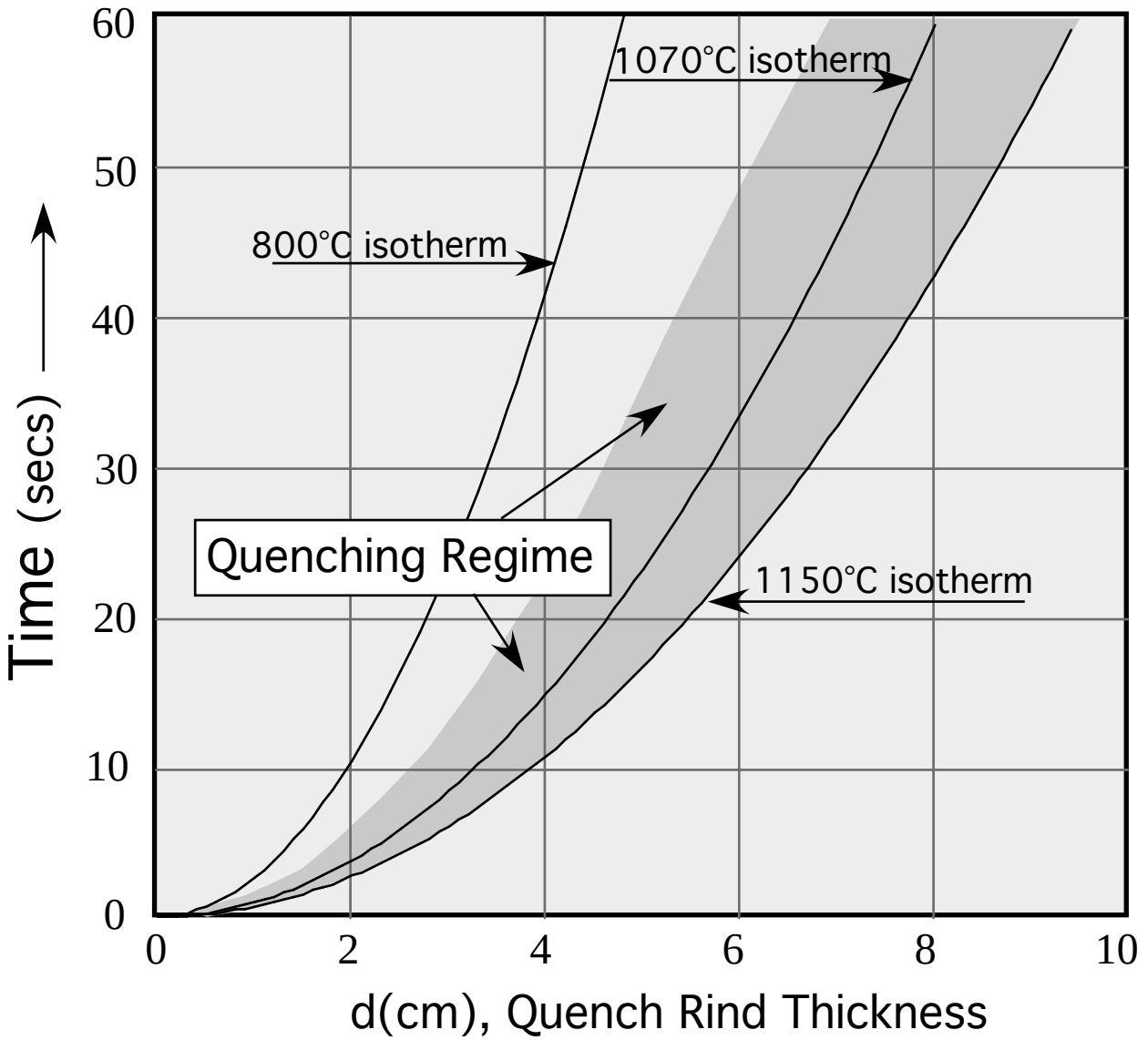
60
50
40
30
20
10
0
Time (secs)
1070°C isotherm
800°C isotherm
Quenching Regime
1150°C isotherm
0
2
4
6
8
10
d(cm), Quench Rind Thickness

Figure 6

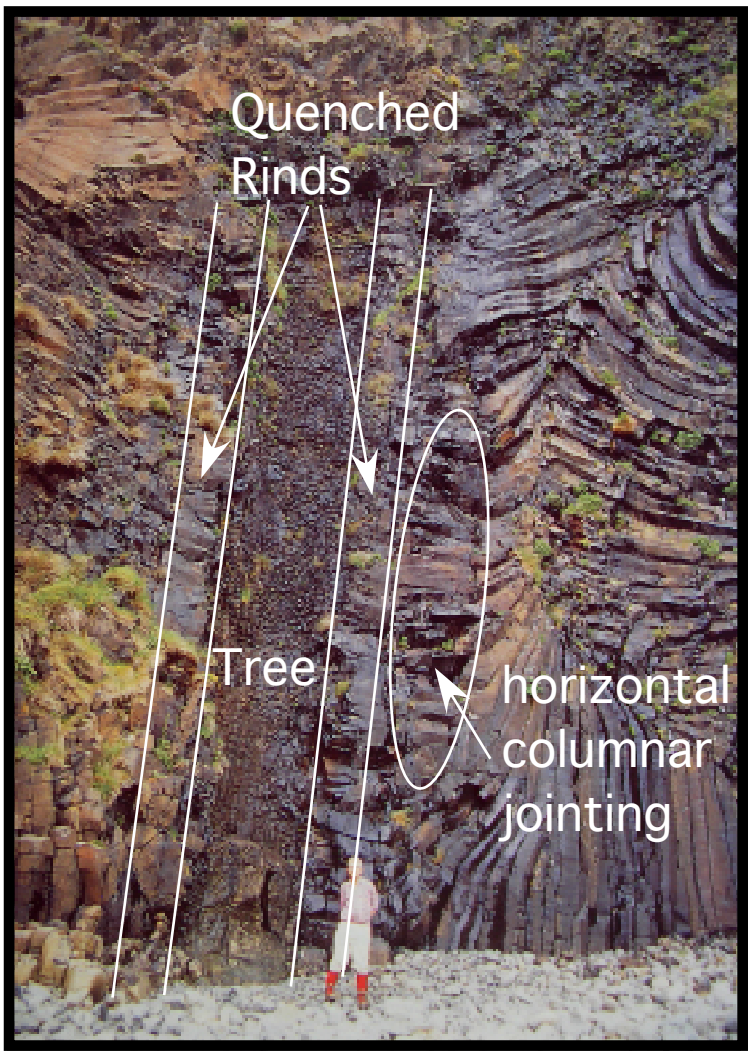

Figure 7

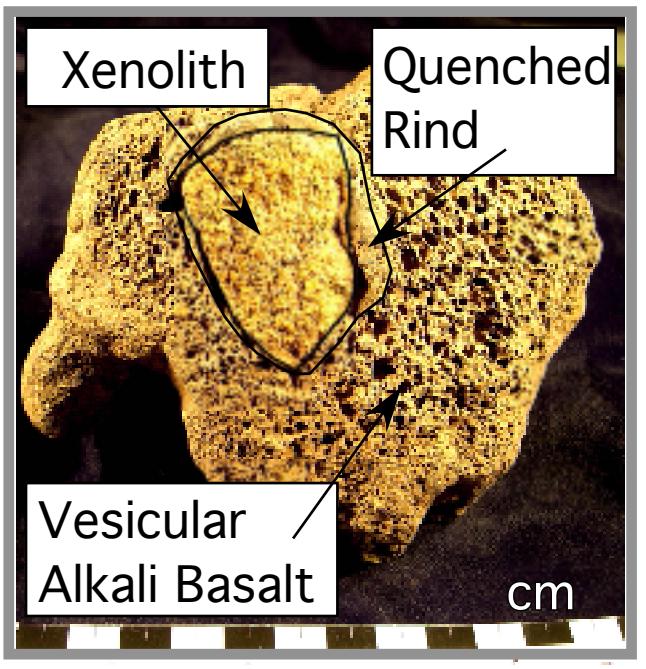

Figure 8

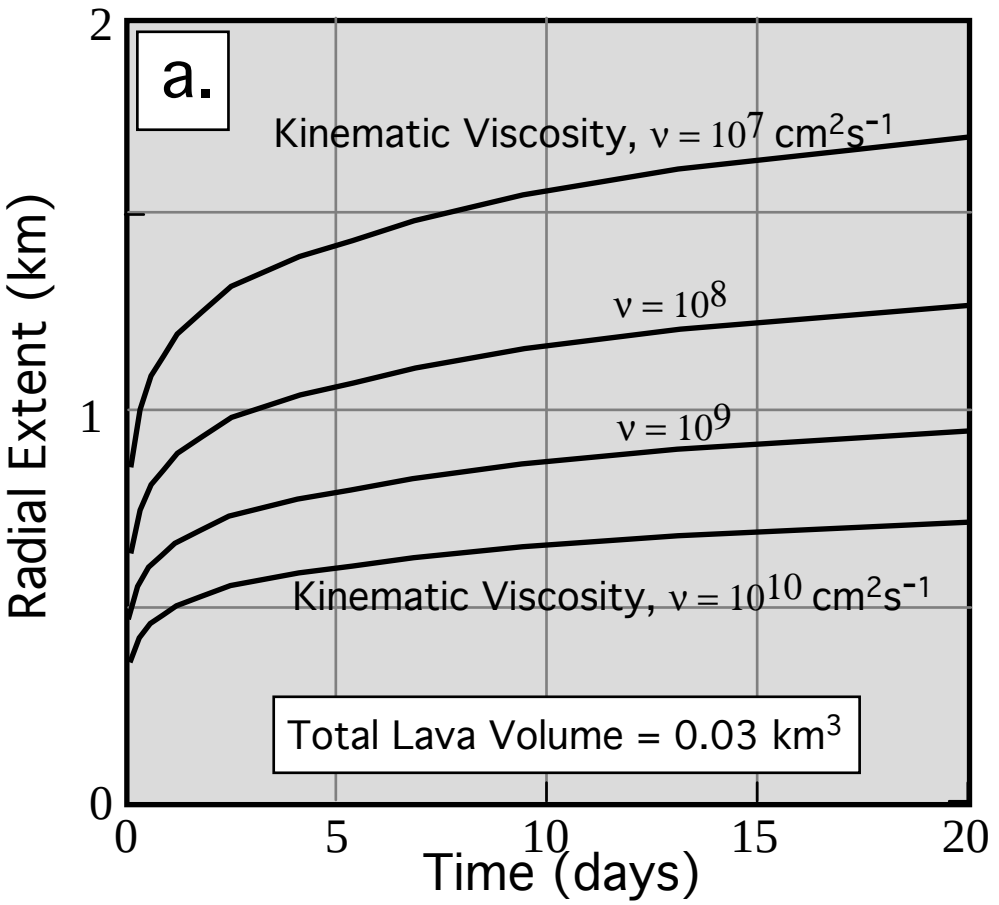
a.
Kinematic Viscosity, ν = 10^7 cm^2s^-1
ν = 10^8
ν = 10^9
Kinematic Viscosity, ν = 10^10 cm^2s^-1
Total Lava Volume = 0.03 km^3
Radial Extent (km)
Time (days)
0
1
2
0
5
10
15
20

Figure 9a

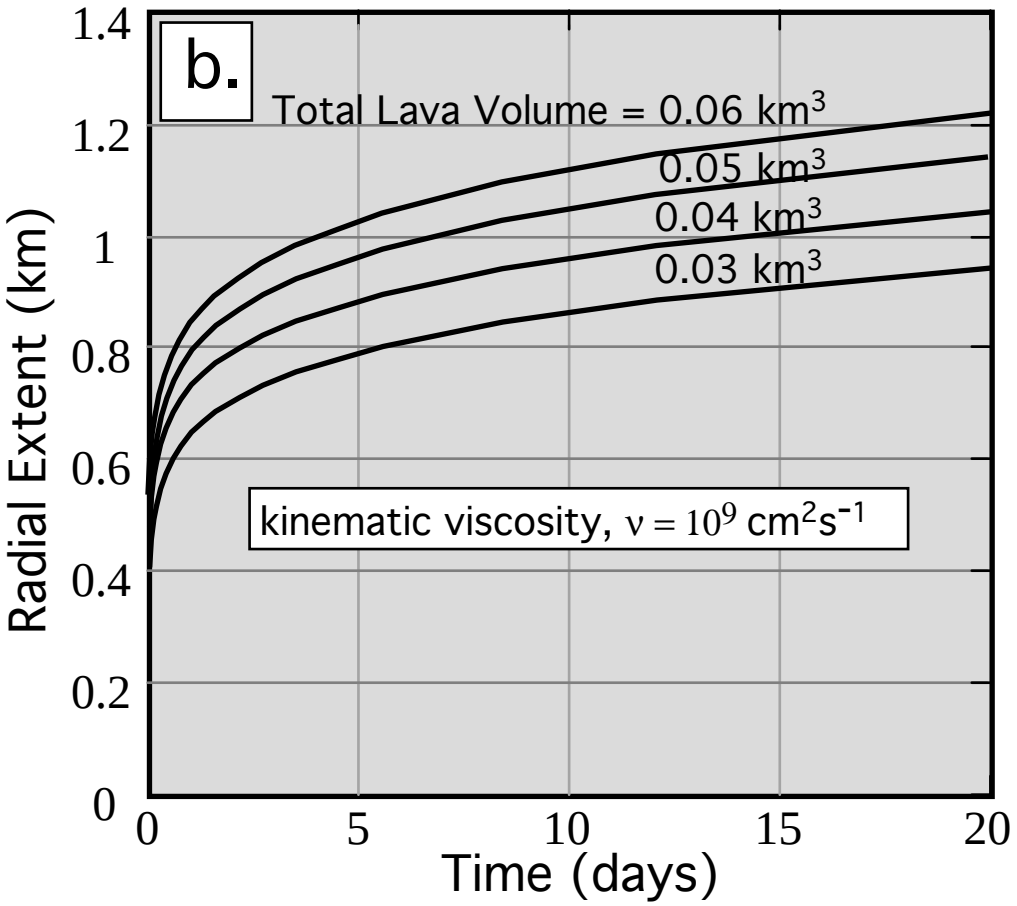
b.
Total Lava Volume = 0.06 km3
0.05 km3
0.04 km3
0.03 km3
kinematic viscosity, ν = 10^9 cm2s-1
Radial Extent (km)
Time (days)
0
0.2
0.4
0.6
0.8
1
1.2
1.4
0
5
10
15
20

Figure 9b

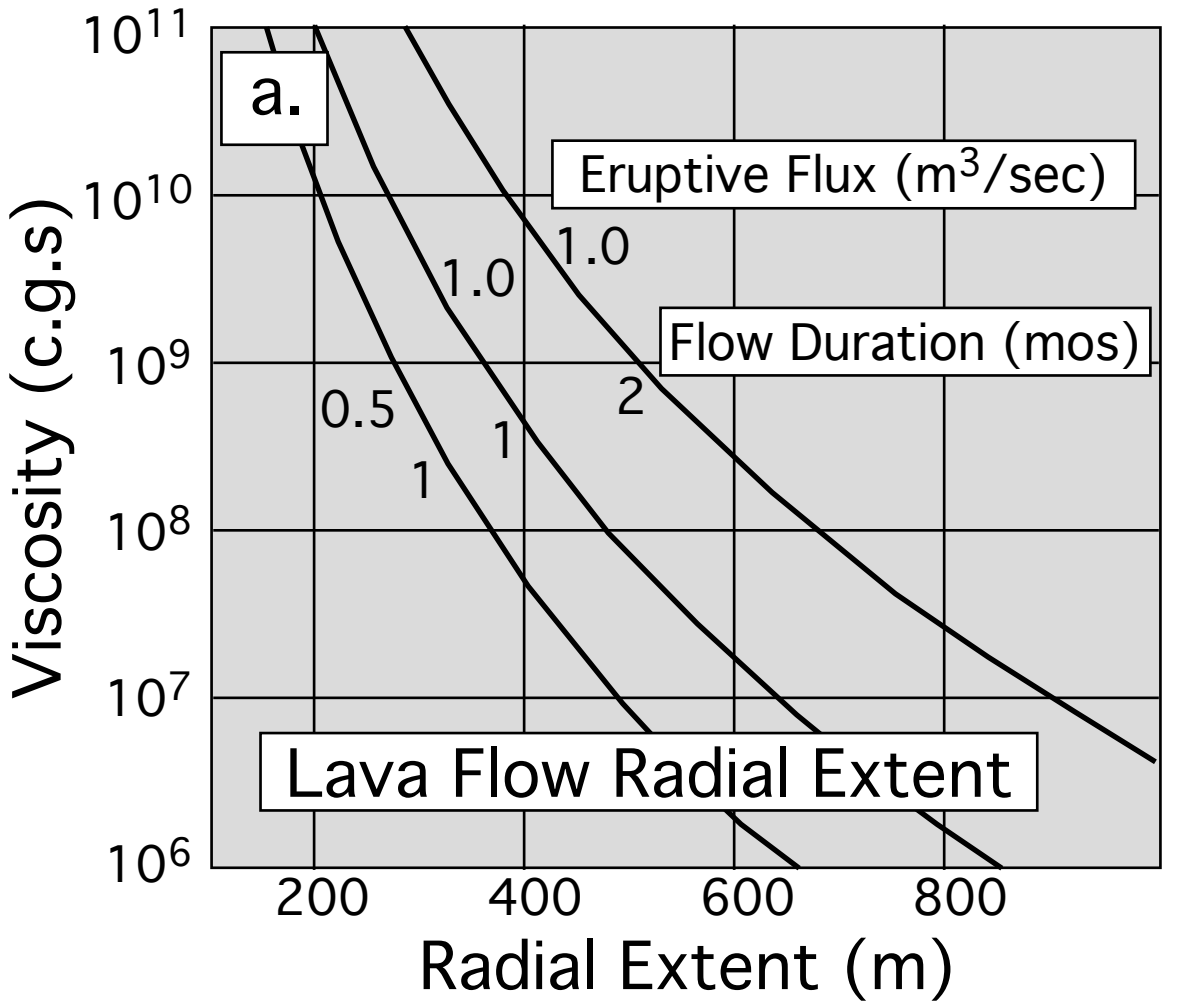
a.
Eruptive Flux (m^3/sec)
1.0
1.0
Flow Duration (mos)
2
0.5
1
1
Lava Flow Radial Extent
Viscosity (c.g.s)
10^{11}
10^{10}
10^9
10^8
10^7
10^6
200
400
600
800
Radial Extent (m)

Figure 10a

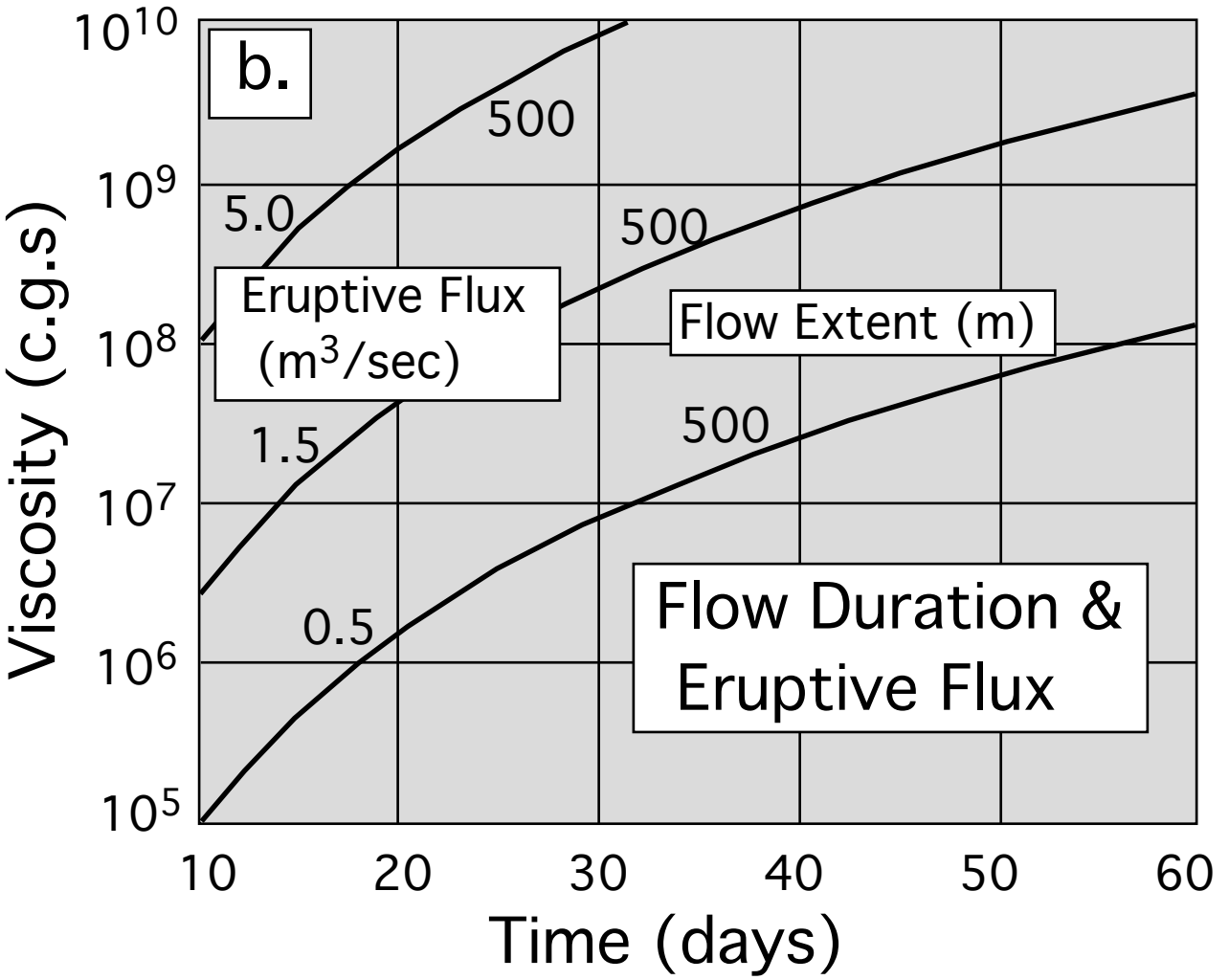
b.
10^{10}
10^{9}
10^{8}
10^{7}
10^{6}
10^{5}
Viscosity (c.g.s)
500
5.0
500
Eruptive Flux
(m^3/sec)
Flow Extent (m)
1.5
500
0.5
Flow Duration &
Eruptive Flux
10
20
30
40
50
60
Time (days)

Figure 10b

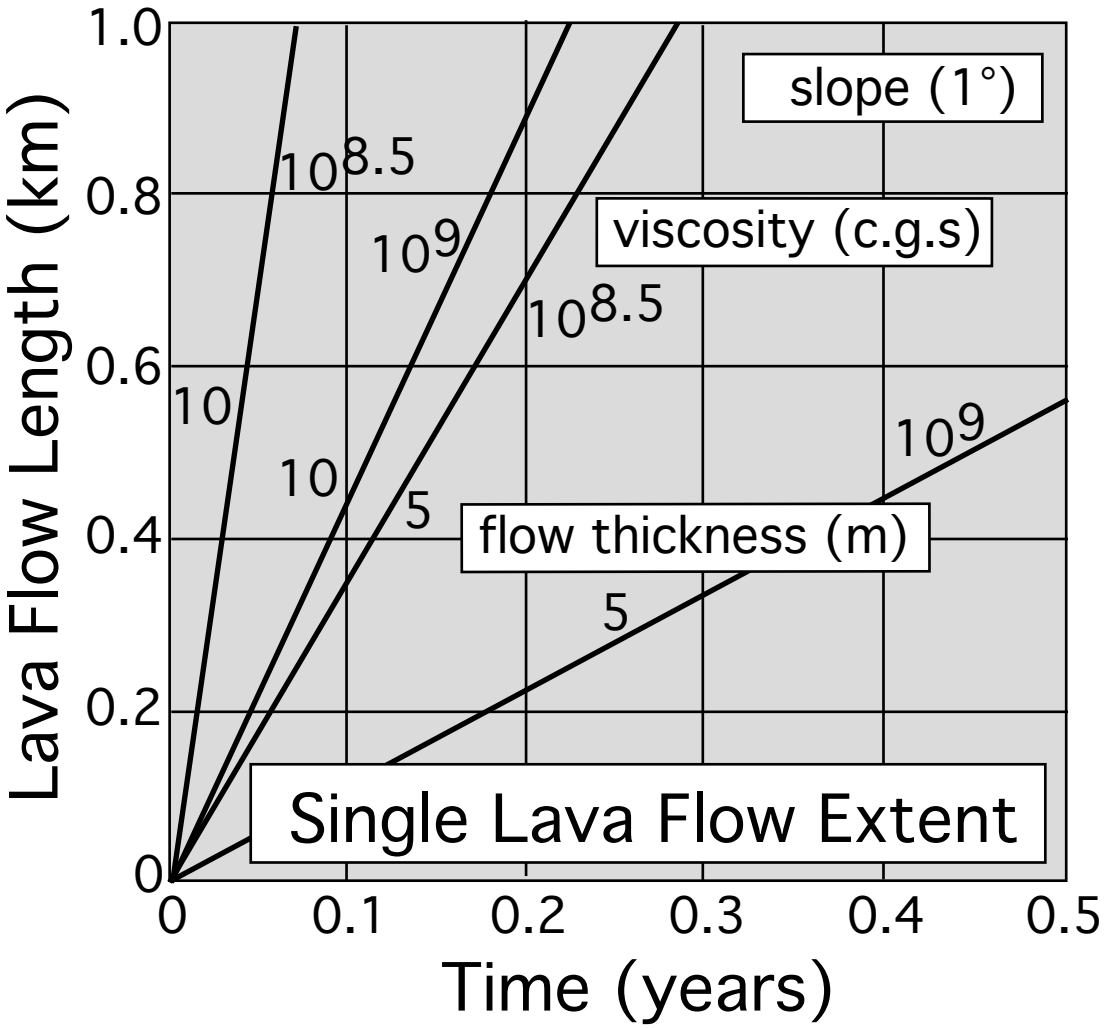
Lava Flow Length (km)
1.0
0.8
0.6
0.4
0.2
0
0
0.1
0.2
0.3
0.4
0.5
Time (years)
slope (1°)
viscosity (c.g.s)
10^8.5
10^9
10^8.5
10
10
5
10^9
flow thickness (m)
5
Single Lava Flow Extent

Figure 11

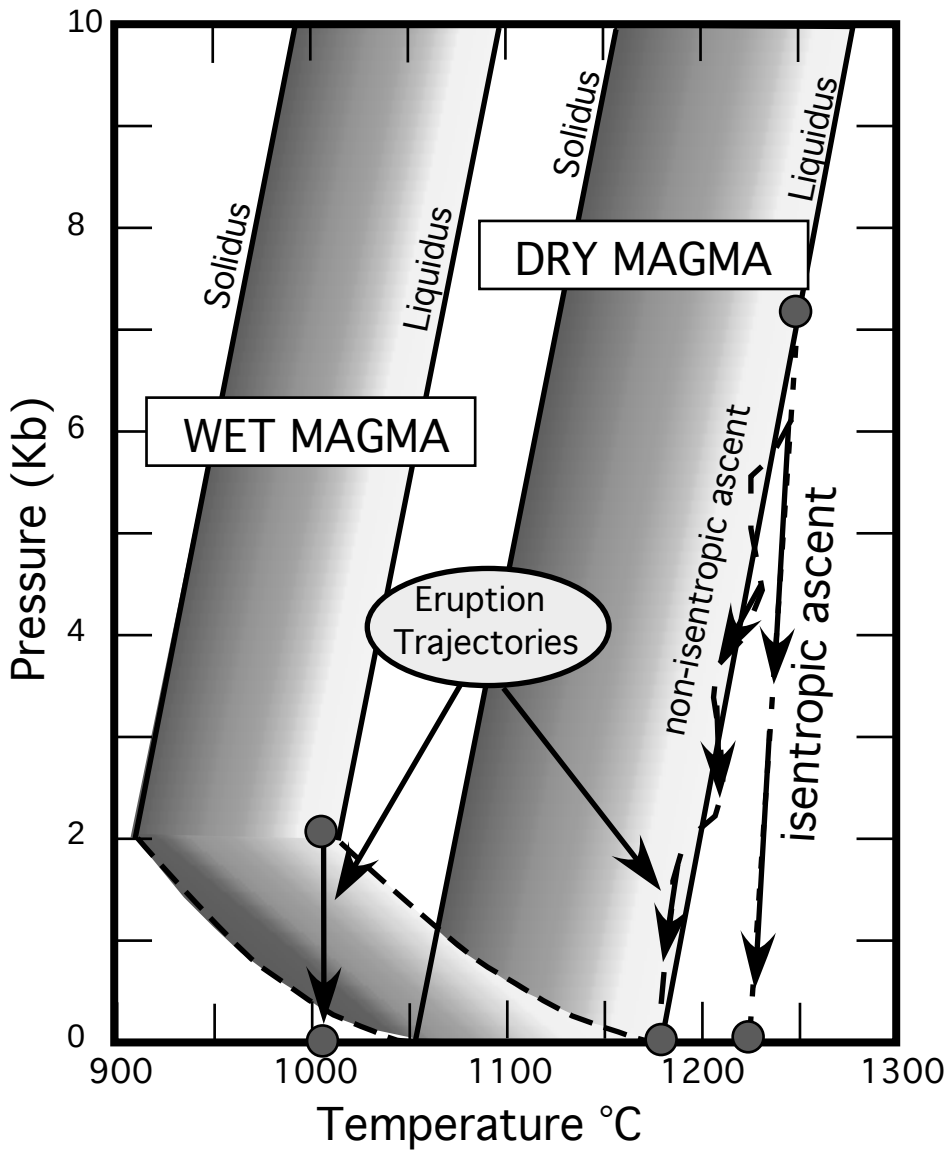
10
8
6
4
2
0
Pressure (Kb)
900
1000
1100
1200
1300
Temperature °C
Solidus
Liquidus
Solidus
Liquidus
DRY MAGMA
WET MAGMA
Eruption
Trajectories
non-isentropic ascent
isentropic ascent

Figure 12

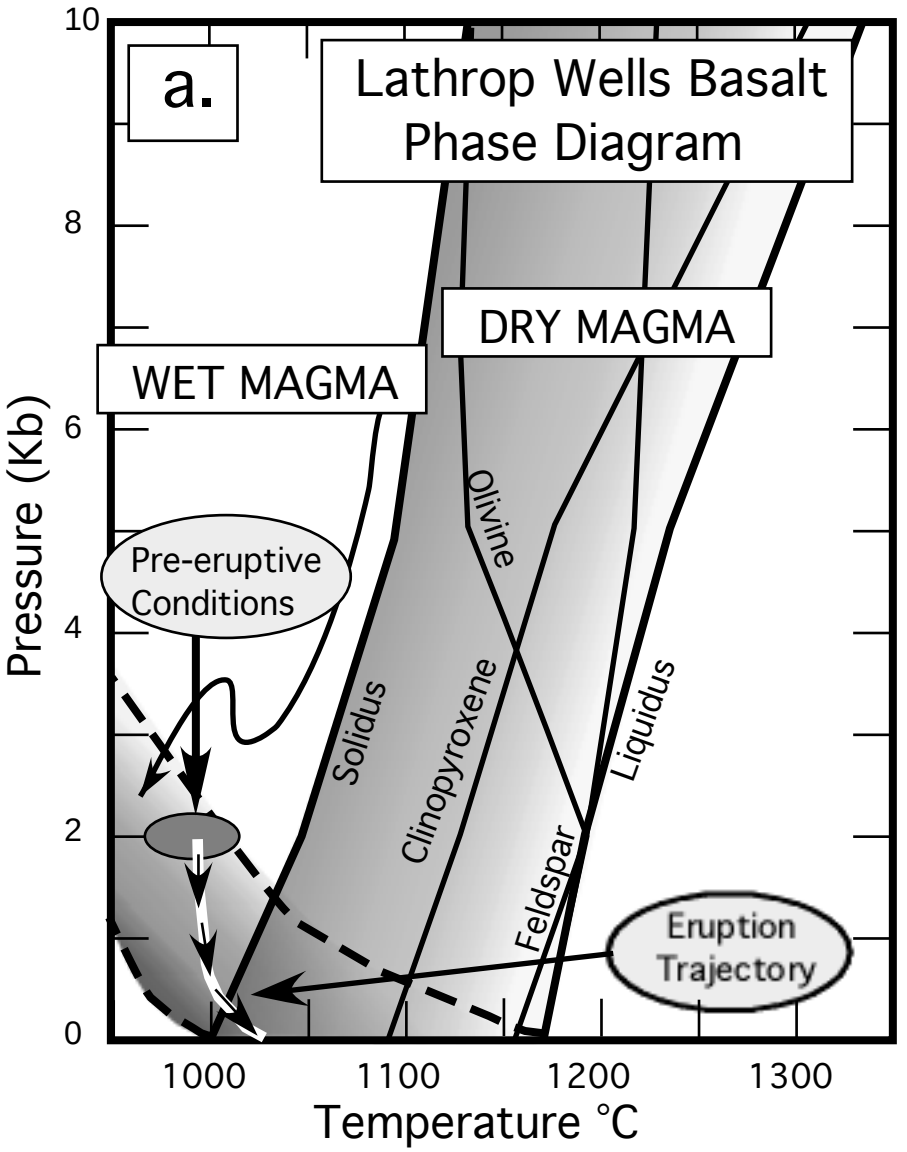
a.
Lathrop Wells Basalt
Phase Diagram
DRY MAGMA
WET MAGMA
Pre-eruptive
Conditions
Olivine
Solidus
Clinopyroxene
Liquidus
Feldspar
Eruption
Trajectory
Pressure (Kb)
Temperature °C
10
8
6
4
2
0
1000
1100
1200
1300

Figure 13a

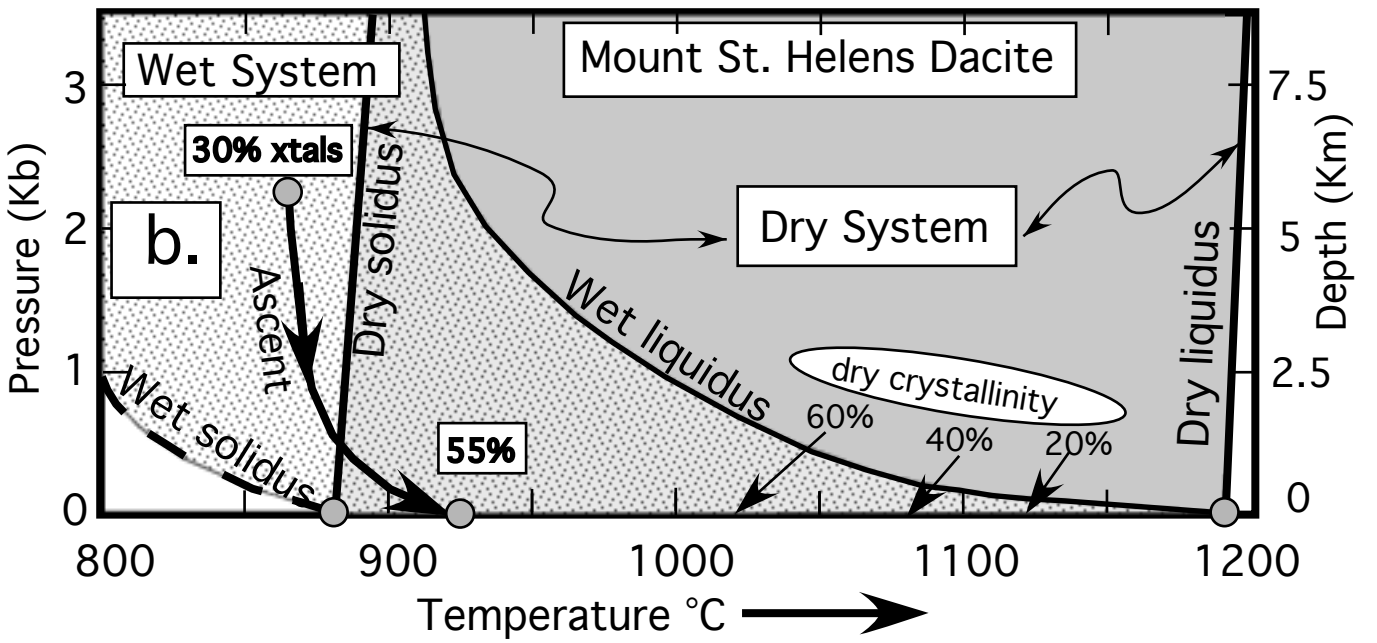
Wet System
Mount St. Helens Dacite
30% xtals
b.
Dry System
Ascent
Dry solidus
Wet liquidus
Dry liquidus
dry crystallinity
60%
40%
20%
Wet solidus
55%
Pressure (Kb)
Depth (Km)
Temperature °C
0
1
2
3
2.5
5
7.5
800
900
1000
1100
1200

Figure 13b

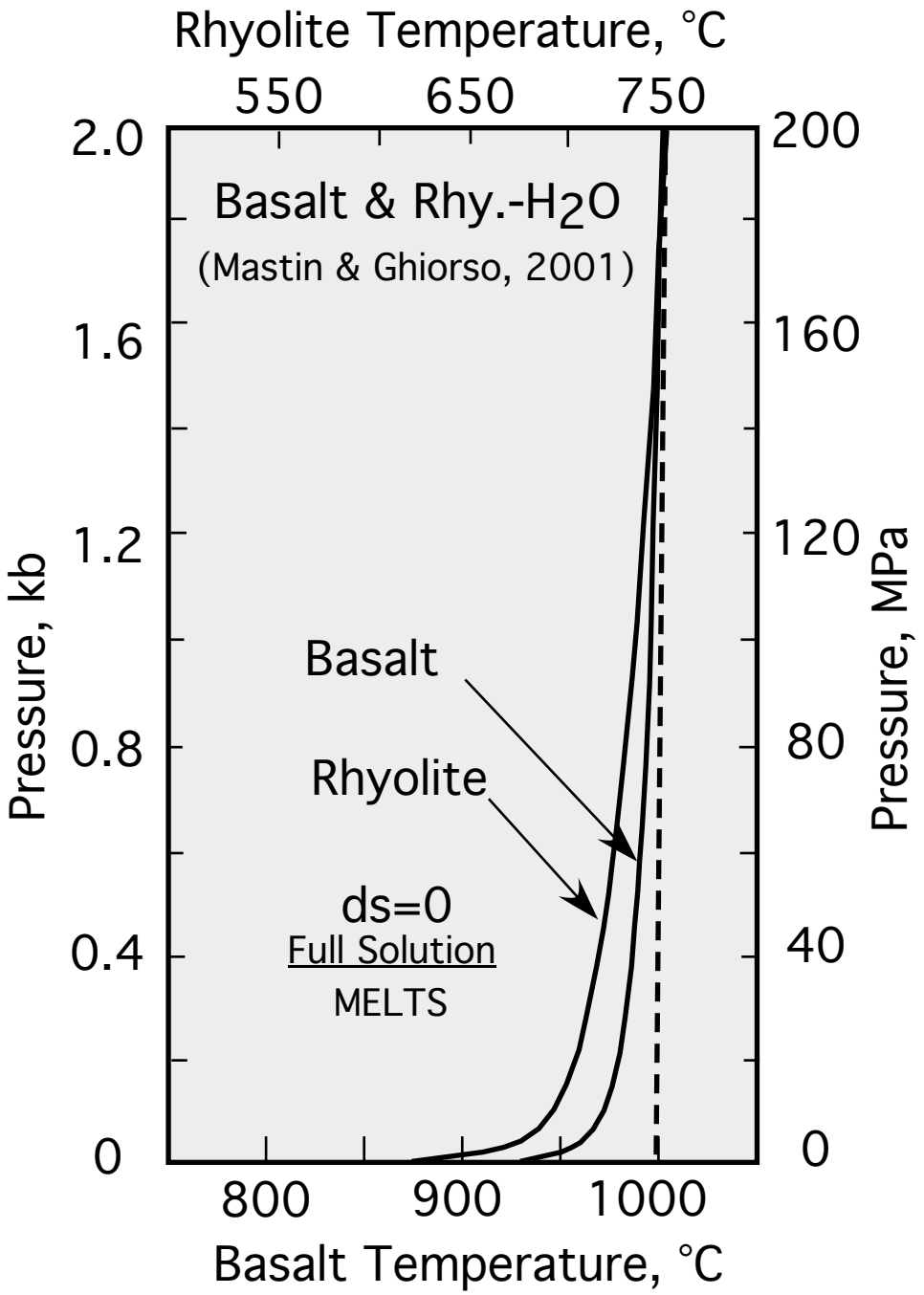
Rhyolite Temperature, °C
550
650
750
2.0
1.6
1.2
0.8
0.4
0
200
160
120
80
40
0
Basalt & Rhy.-H2O
(Mastin & Ghiorso, 2001)
Basalt
Rhyolite
ds=0
Full Solution
MELTS
Pressure, kb
Pressure, MPa
800
900
1000
Basalt Temperature, °C

Figure 14

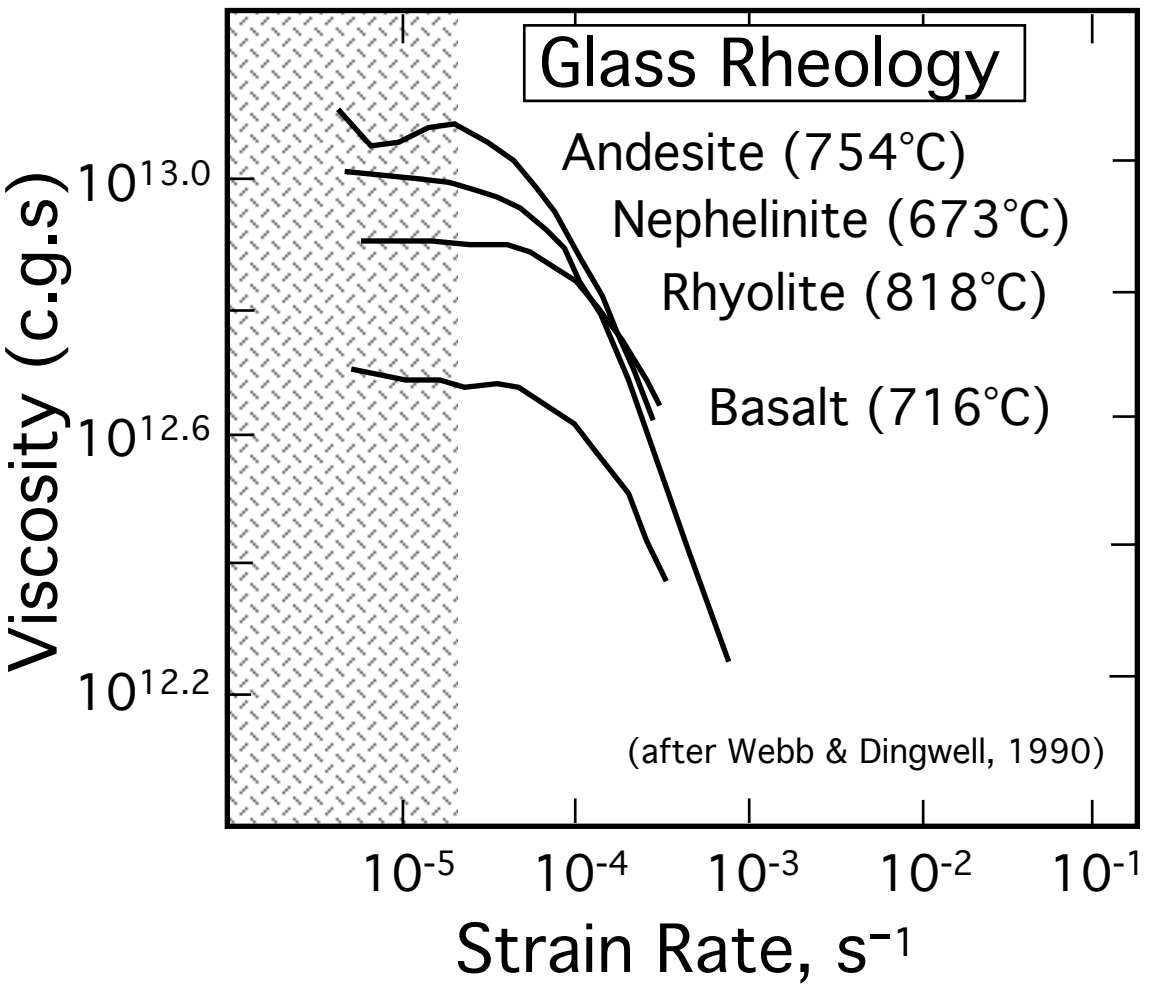
Glass Rheology
Andesite (754°C)
Nephelinite (673°C)
Rhyolite (818°C)
Basalt (716°C)
(after Webb & Dingwell, 1990)
Viscosity (c.g.s)
10^13.0
10^12.6
10^12.2
10^-5
10^-4
10^-3
10^-2
10^-1
Strain Rate, s^-1

Figure 15

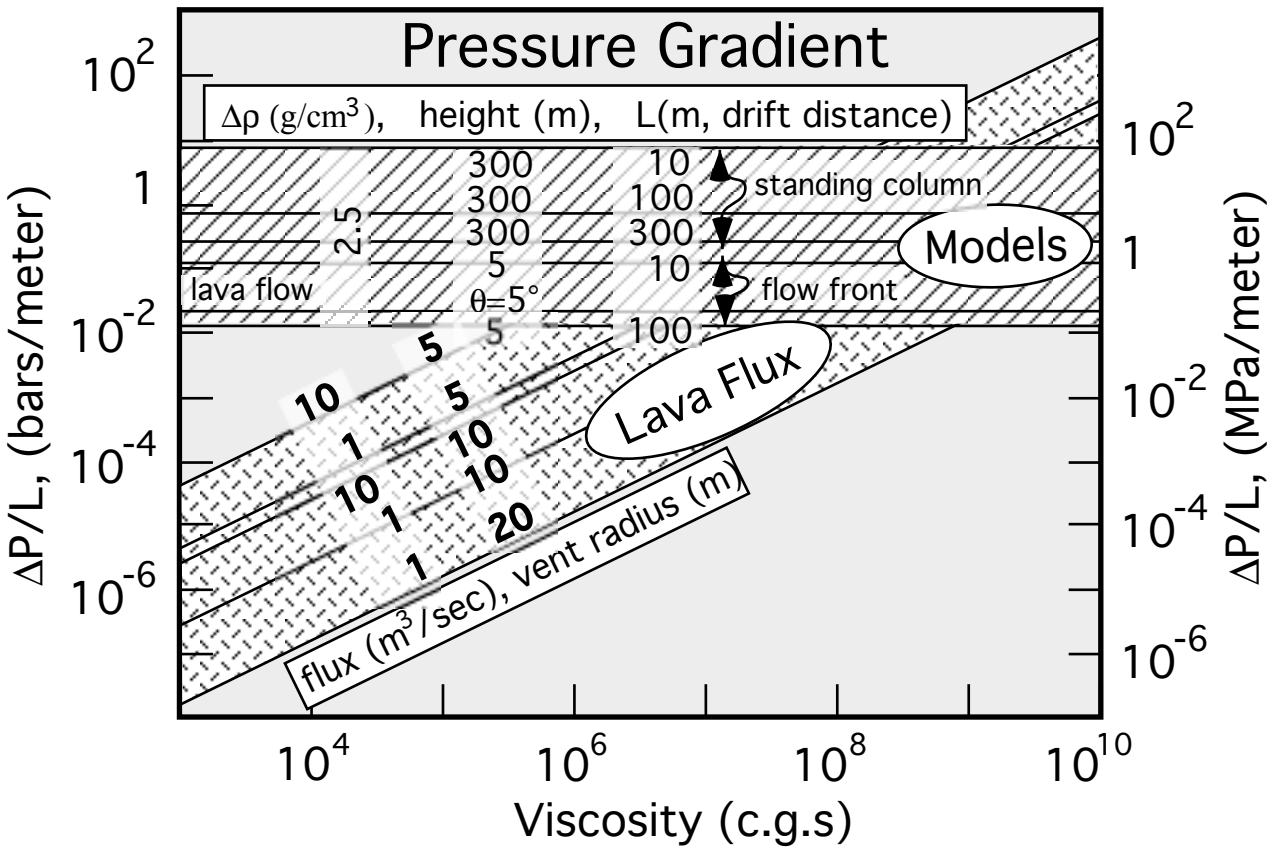
Pressure Gradient
Δρ (g/cm3), height (m), L(m, drift distance)
300
300
300
5
θ=5°
5
2.5
10
100
300
10
100
standing column
Models
flow front
lava flow
Lava Flux
flux (m3/sec), vent radius (m)
5
10
1
10
5
10
1
10
1
20
ΔP/L, (bars/meter)
ΔP/L, (MPa/meter)
10^2
1
10^-2
10^-4
10^-6
10^4
10^6
10^8
10^10
Viscosity (c.g.s)

Figure 16

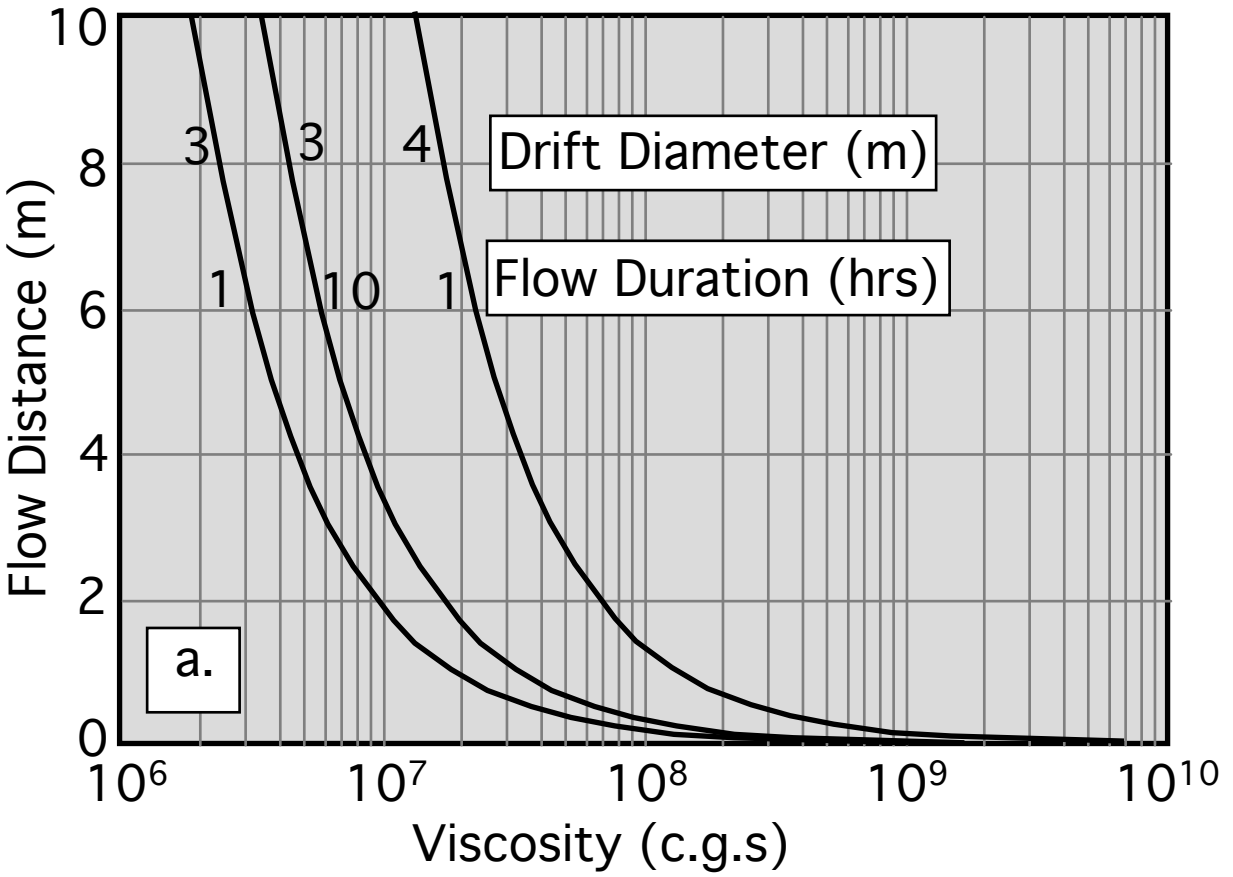
10
8
6
4
2
0
Flow Distance (m)
3
3
4
Drift Diameter (m)
1
10
1
Flow Duration (hrs)
a.
10^6
10^7
10^8
10^9
10^10
Viscosity (c.g.s)

Figure 17a

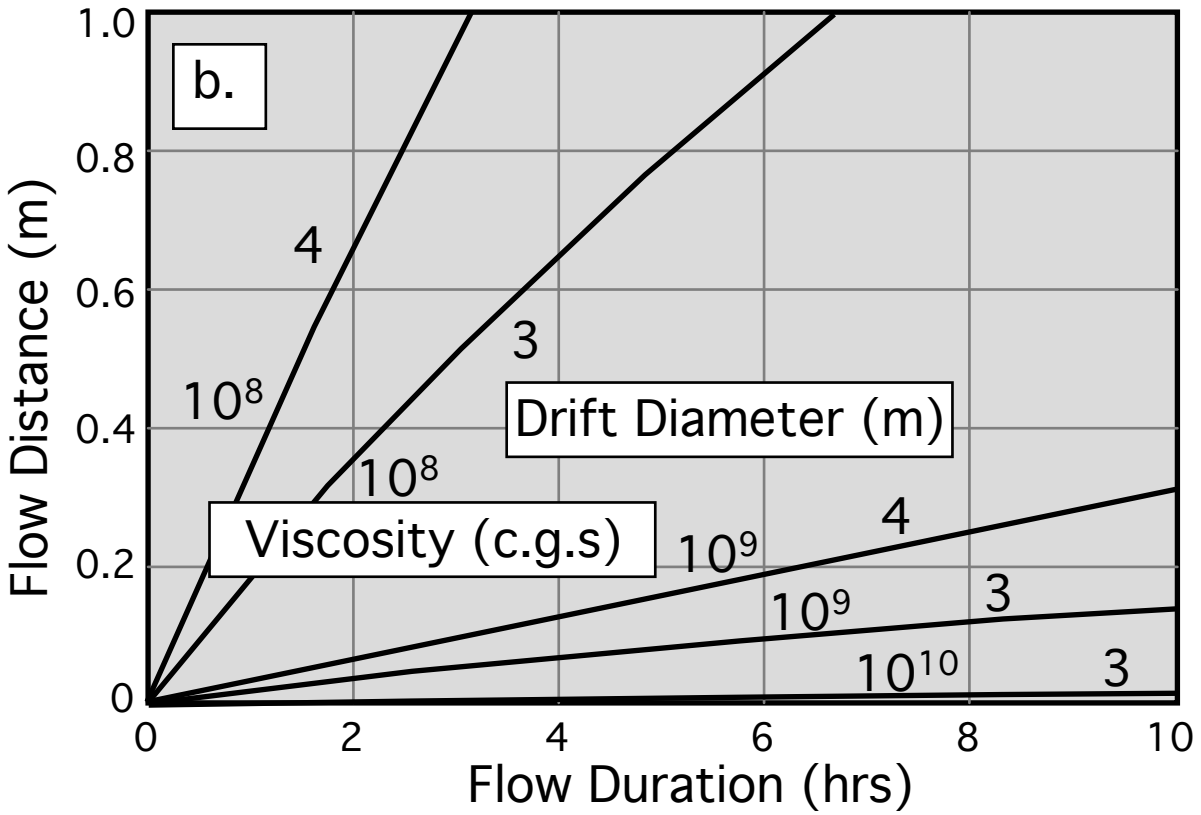
b.
Flow Distance (m)
Flow Duration (hrs)
1.0
0.8
0.6
0.4
0.2
0
0
2
4
6
8
10
4
3
10^8
10^8
Drift Diameter (m)
Viscosity (c.g.s)
10^9
4
10^9
3
10^{10}
3

Figure 17b

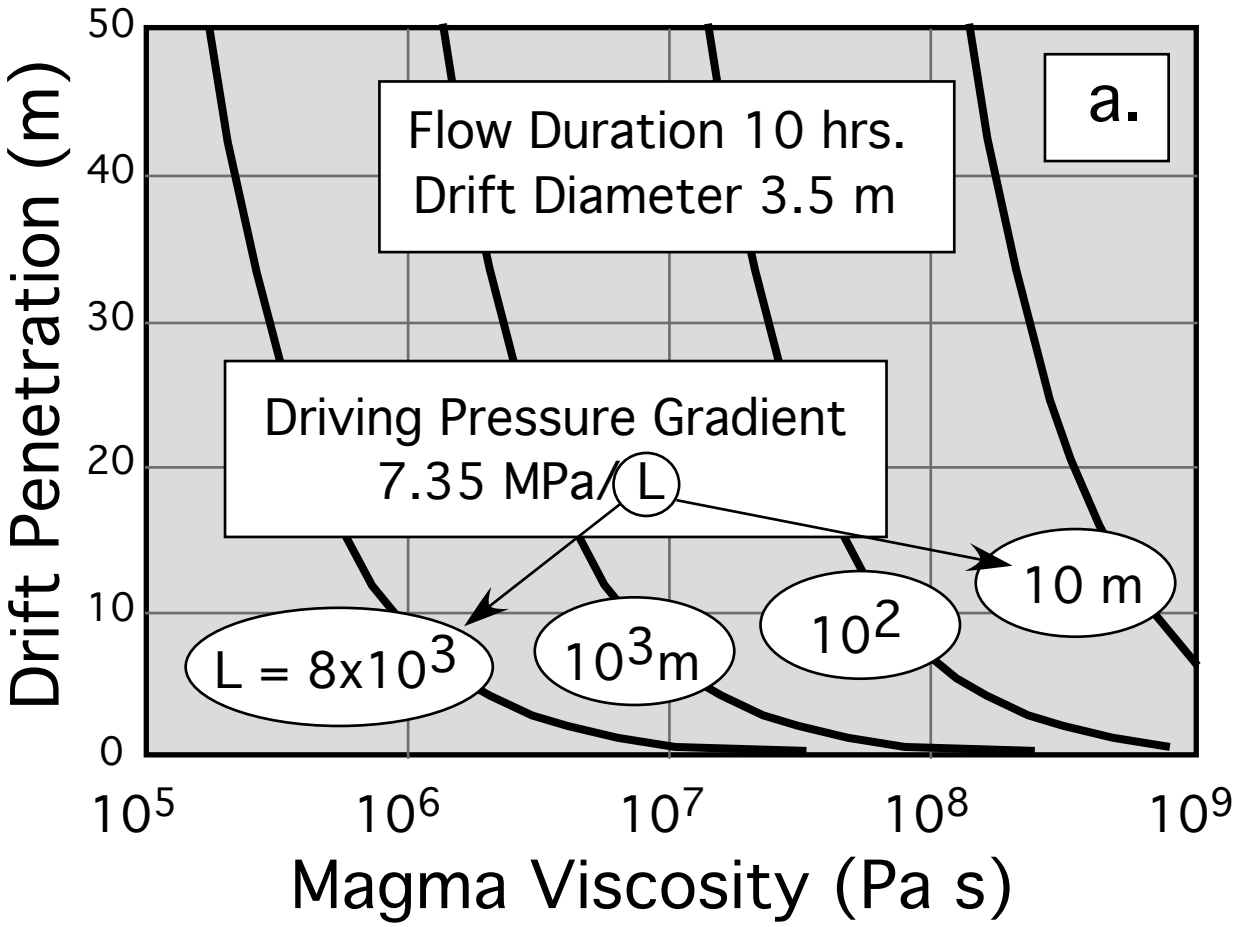
a.
Flow Duration 10 hrs.
Drift Diameter 3.5 m
Driving Pressure Gradient
7.35 MPa/ L
L = 8x10^3
10^3m
10^2
10 m
Drift Penetration (m)
0
10
20
30
40
50
10^5
10^6
10^7
10^8
10^9
Magma Viscosity (Pa s)

Figure 18a

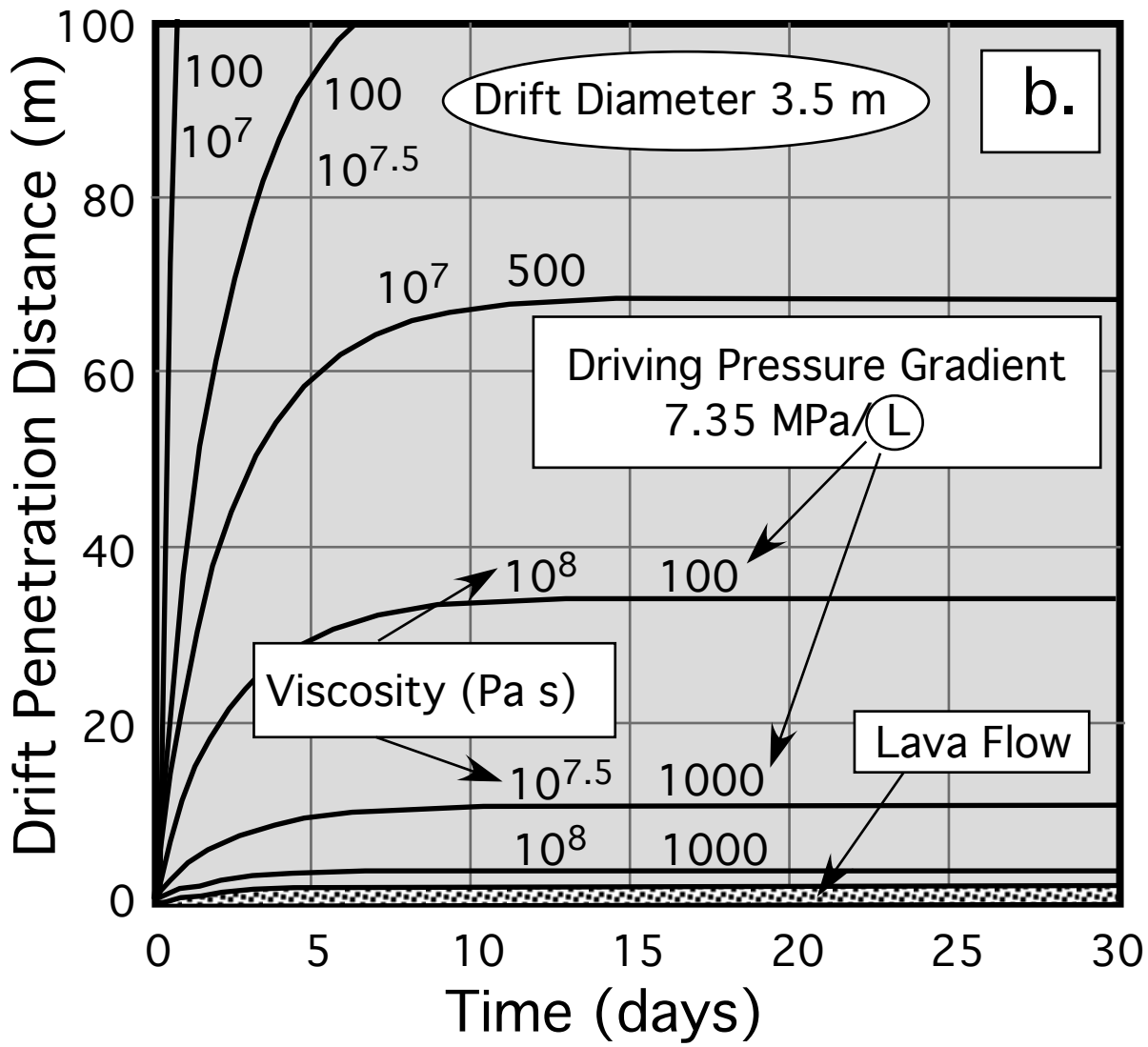
Drift Penetration Distance (m)
Time (days)
Drift Diameter 3.5 m
b.
100
10^7
100
$10^{7.5}$
10^7
500
Driving Pressure Gradient
7.35 MPa/L
10^8
100
Viscosity (Pa s)
Lava Flow
$10^{7.5}$
1000
10^8
1000
0
20
40
60
80
100
0
5
10
15
20
25
30

Figure 18b

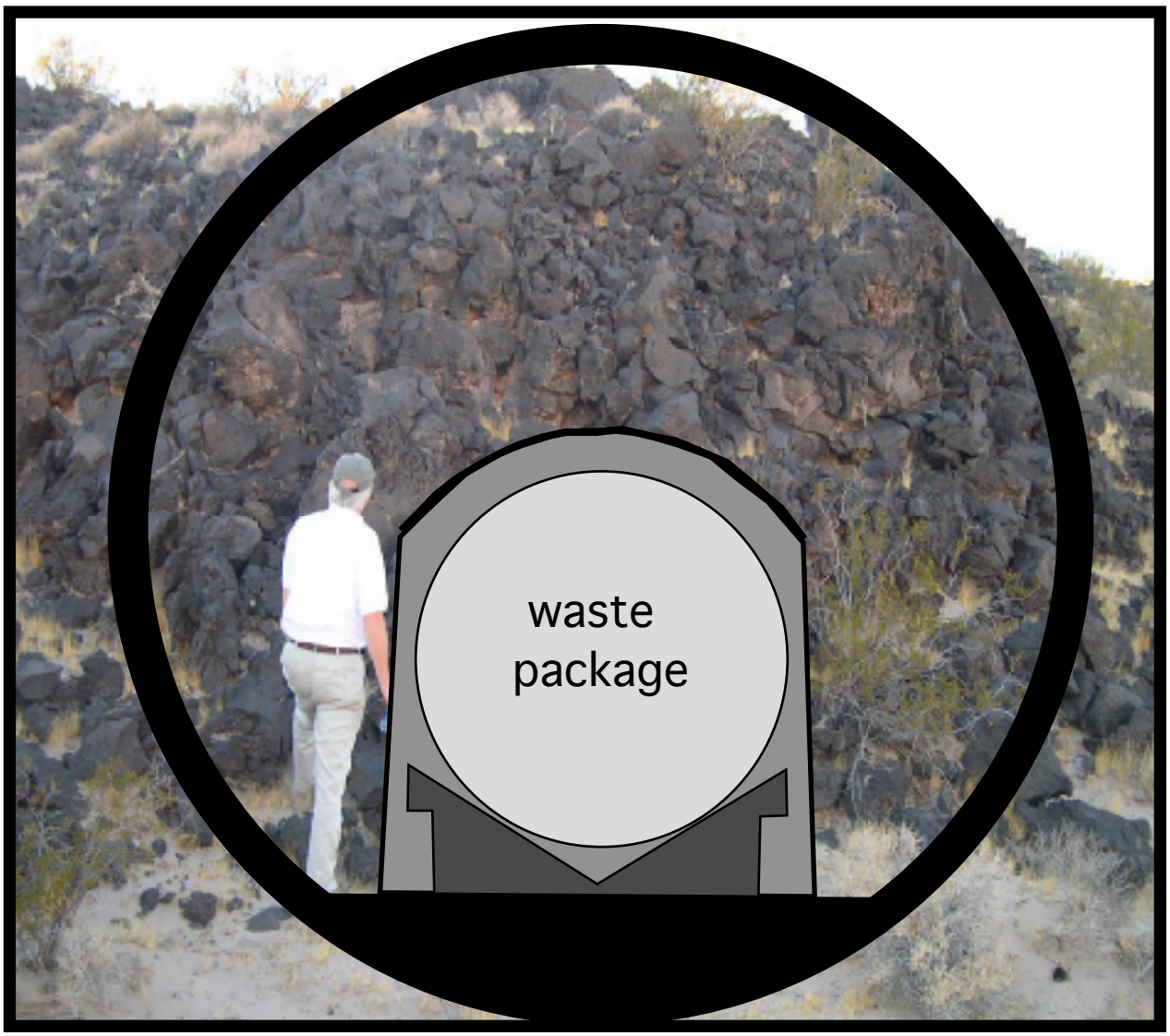

Figure 19